

# A Bregman-Sinkhorn Algorithm for the Maximum Weight Independent Set Problem

Stefan Haller\*, Bogdan Savchynskyy

Heidelberg University

## Abstract

We propose a scalable approximate algorithm for the NP-hard maximum-weight independent set problem. The core of our algorithm is a dual coordinate descent applied to a smoothed LP relaxation of the problem. This technique is referred to as *Bregman method* or *Sinkhorn algorithm* in the literature. Our algorithm addresses a family of *clique cover LP relaxations*, where the constraints are determined by the set of cliques covering the underlying graph. The objective function of the relaxation is smoothed with an entropy term.

An important question determining efficiency of our algorithm is the control of the smoothing level over the course of optimization. While several dedicated techniques have been considered in the literature to this end, we propose a new one based on estimation of the relaxed duality gap. To make this estimation possible, we developed a new projection method to the feasible set of the considered LP relaxation. We experimentally show that our technique notably outperforms the standard one based on feasibility estimation.

Additionally to solving the relaxed dual, we utilize a simple and very efficient primal heuristic to obtain feasible integer solutions of the initial non-relaxed problem. Our heuristic is a combination of the greedy generation and optimal recombination applied to the reduced costs computed by the dual optimization.

Our experimental validation considers two datasets based on real-life applications, where our method shows competitive results being able to find high quality approximate solutions within 10 seconds for graphs with hundreds of thousands of nodes and dozens of millions of edges.

## 1 Introduction

Let  $\mathcal{G} = (\mathcal{V}, \mathcal{E})$  be a undirected graph with a *node set*  $\mathcal{V}$  and an *edge set*  $\mathcal{E} \subseteq \binom{\mathcal{V}}{2}$ . An *independent* or *stable set* is the subset of mutually non-adjacent vertices  $\mathcal{V}' \subseteq \mathcal{V}$ ,

\* This research was partially conducted during the author's employment at rabbitAI GmbH.

e.g., for any  $i, j \in \mathcal{V}'$  it holds  $\{i, j\} \notin \mathcal{E}$ . Given the costs  $c_i, i \in \mathcal{V}$ , the *maximum weight independent set* (MWIS) problem consists in finding an independent set with the maximum total cost.

The problem has applications in computer vision [5], [27, Ch.7], vehicle routing [8], transmission scheduling in wireless networks [32] and is one of the classical combinatorial optimization problems [11]. It is NP-hard, since its unweighted variant is NP-complete [19].<sup>1</sup>

Therefore, different relaxations and approximate algorithms addressing it have been proposed.

We consider a family of *clique cover relaxations* for this problem and propose a scalable dual algorithm. We augment it with an efficient primal heuristic that profits from the reduced costs computed by the dual algorithm. In total, this leads to an efficient and well-scalable MWIS method.

**Notation.** Vectors are **bold** and scalars not:  $\mathbf{x}$  is a vector and  $x$  is a scalar. Scalar operations and relations are applied to vectors component-wise:  $\mathbf{x} \geq \mathbf{0}$  means non-negativity of all coordinates of  $\mathbf{x}$  and  $\log \mathbf{x}$  is a vector of coordinate logarithms.  $\mathbb{R}_{\geq 0}^n := \{x \in \mathbb{R}: x \geq 0\}$ ,  $[n] := \{1, 2, \dots, n\}$ .  $\llbracket A \rrbracket$  are Iverson brackets equal to 1 if  $A$  holds, otherwise 0.

*Notation introduced further in the paper:*  $\mathbf{x}$  - primal variables,  $\mathbf{c}$  - cost vector (Section 1);  $\lambda$  - dual variables,  $\mathbf{c}^\lambda$  - vector of reduced costs (Section 4);

$\bar{K}_j = K_j \cup \{x_{n+j}\}$ ,  $j \in [m]$ , are cliques with and without slack variables  $x_{n+j}$  (Section 1);

$C = \{x \in [0, 1]^{n+m}: \sum_{i \in \bar{K}_j} x_i = 1, j \in [m]\}$  is a feasible set of the relaxed problem (3) (Section 7.3).

## 2 Overview of the known results and related work

The MWIS problem is also known as *maximum weight stable set* or *vertex packing* and is mutually reducible to the *minimum weight vertex cover*, *maximum weight clique* and *weighted set packing* problems [16, 9]. Algorithms

<sup>1</sup> The vertex cover problem, reducible to MWIS, is considered.

addressing these problems can be *straightforwardly* applied to MWIS and vice versa. Many theoretical results are shared by these problems as well. Yet, we will stick to the MWIS problem formulation in the following.

**ILP formulation and edge relaxation.** Let  $[n]$  stand for  $\{1, 2, \dots, n\}$  and assume that the set of graph nodes has  $n$  elements, i.e.,  $\mathcal{V} = [n]$ . Introduce a binary variable  $x_i \in \{0, 1\}$  for each node  $i \in \mathcal{V}$ . Its value 1 denotes that the respective node belongs to the maximum-weight independent set. This leads to a natural integer linear program (ILP) formulation of the MWIS problem:

$$\begin{aligned} & \max_{\mathbf{x} \in \{0,1\}^n} \langle \mathbf{c}, \mathbf{x} \rangle \\ \text{s.t. } & x_i + x_j \leq 1, \{i, j\} \in \mathcal{E}. \end{aligned} \quad (1)$$

The respective LP relaxation, obtained by substituting the integer constraints  $\mathbf{x} \in \{0, 1\}^n$  with the box constraints  $\mathbf{x} \in [0, 1]^n$ , is referred to as the *edge relaxation*. It is well-known that it is tight for bipartite graphs [23] and can be reduced to min-st-cut/max-flow and thus efficiently solved [23, 16]. The efficient solvability of the edge relaxation follows from its two interrelated properties [23]: First, the respective polytope has only *half-integral* vertices, that is, all basic solutions of the relaxation have coordinates from the set  $\{0, 1, 1/2\}$ . The second is the *persistency* property: All coordinates of a relaxed solution with integer (0 or 1) values belong to some (and the same) optimal solution of the non-relaxed problem (1). In particular, the persistency property has been used to improve approximation bounds of several primal heuristics, see e.g., [16, 17].

However, the edge relaxation has also its limitations: It gets loose for dense graphs, as demonstrated by the following example:

**Proposition 1.** *Let  $G$  be fully-connected, all costs positive,  $c_j > 0, j \in \mathcal{V}$ , and  $c_i < \sum_{j \in \mathcal{V} \setminus \{i\}} c_j$  for  $i = \arg \max_{j \in \mathcal{V}} c_j$ .*

*Then the edge relaxation has a unique solution  $(\underbrace{\frac{1}{2}, \frac{1}{2}, \dots, \frac{1}{2}}_n)$ .*

Note that costs positivity can be assumed w.l.o.g. for the MWIS problem. Nodes with non-positive costs can be excluded from the graph together with their incident edges without influencing the optimal objective value.

Proposition 1, proved in Section 13 together with all other statements, shows that the edge relaxation may not reveal *any* information about optimal solutions of the non-relaxed problem (1) for dense graphs. To address this limitation, the *clique constraints* and the respective *clique relaxation* are considered for the MWIS problem in the literature [30], [36, Sec.64]. Before defining it, we first introduce a family of relaxations that includes both the edge and the clique relaxations.

**Clique cover relaxation family.** Let  $K_j \subseteq \mathcal{V}, j \in [m]$ , be subsets of the nodes such that the respective induced subgraphs of  $G$  are cliques. Abusing notation, we will refer to  $K_j$  themselves as *cliques*. We assume that  $K_j, j \in [m]$ , cover all edges and nodes of the graph, e.g.  $\mathcal{E} = \bigcup_{j=1}^m \{\{i, i'\} : i, i' \in K_j\}$ ,  $\mathcal{V} = \bigcup_{j=1}^m \{i : i \in K_j\}$ , and, therefore, are referred to as a *clique cover*.<sup>2</sup> We define the *clique cover ILP formulation* of the MWIS problem as

$$\begin{aligned} & \max_{\mathbf{x} \in \{0,1\}^n} \langle \mathbf{c}, \mathbf{x} \rangle \\ \text{s.t. } & \sum_{i \in K_j} x_i \leq 1, j \in [m]. \end{aligned} \quad (2)$$

Its natural LP relaxation, further referred to as *clique cover relaxation* is obtained by substituting integer constraints  $\mathbf{x} \in \{0, 1\}^n$  with the respective box constraints  $\mathbf{x} \in [0, 1]^n$ . The relaxation (3) is called *clique relaxation*, if the set  $\{K_j : j \in [m]\}$ , consists of *all* cliques of  $G$ .

Whereas the solutions of the non-relaxed problems (1) and (2) coincide, their relaxations may differ a lot. In particular, the clique relaxation possess neither the half-integrality nor the persistency property in general [30]. Also, no reduction to any efficiently solvable LP subclass like the min-cost-flow problem is possible for it, as this relaxation is as difficult as linear programs in general [28]. However, it is tighter in general, as shown by the following statement:

**Proposition 2.** *Let  $K_j, j \in [m]$ , and  $K'_j, j \in [m']$ , be two clique covers of the graph  $G$  such that for every  $K'_j, j \in [m']$ , there is  $l \in [m] : K'_j \subseteq K_l$ . Then the relaxation determined by  $K_j, j \in [m]$ , is at least as tight as the relaxation determined by  $K'_j, j \in [m']$ .*

Proposition 2 defines a partial order on the set of clique cover relaxations with respect to their tightness. The edge relaxation is the least tight and constitutes the minimum with respect to this partial order. The maximum is determined by the clique relaxation. According to Proposition 2, the latter is equivalent to the relaxation, where  $K_j, j \in [m]$ , consists of maximal cliques (i.e., those that are not subgraphs of any other clique) only. It is also known that clique inequalities are facet-defining for the stable set polytope<sup>3</sup> if and only if the respective clique is maximal [36].

Considering the same setting as in Proposition 1, one obtains the following result:

**Proposition 3.** *The maximal clique relaxation, defined by the single maximal clique, is tight for complete graphs.*

Unfortunately, the number of maximal cliques may grow exponentially with the graph size in general [22]. Hence in practice one has to ideally consider a clique

<sup>2</sup> The covering of nodes in addition to the covering of edges is required to deal with isolated nodes.

<sup>3</sup> The convex hull of all feasible solutions of (1).

cover consisting of a subset of the maximal cliques, although the algorithms we describe in this paper are applicable to *arbitrary* clique covers.

**Equality formulation.** Note that the clique constraints in (2) can be turned to equality by introducing  $m$  slack variables  $x_{n+j}$ ,  $j \in [m]$ , and assuming  $c_{n+j} = 0$  and  $\bar{K}_j = K_j \cup \{n+j\}$ . The respective LP relaxation takes the form:<sup>4</sup>

$$\begin{aligned} \max_{\mathbf{x} \in [0,1]^{n+m}} & \langle \mathbf{c}, \mathbf{x} \rangle \\ \text{s.t. } & \sum_{i \in \bar{K}_j} x_i = 1, j \in [m]. \end{aligned} \quad (3)$$

As (3) is equivalent to the clique cover relaxation, we will primarily use this name to refer to (3) unless otherwise stated. Likewise, the non-trivial constraints of (3) will be called *clique constraints* just like those in (2). To avoid ambiguity we will reference the specific formula.

**Remark 1.** The box constraints  $\mathbf{x} \in [0, 1]^{n+m}$  in (3) can be substituted with the non-negativity constraints  $\mathbf{x} \geq \mathbf{0}$  without changing the feasible set of the problem. This is because  $\mathbf{x} \leq \mathbf{1}$  due to the clique constraints in (3), as cliques cover all vertices of the underlying graph. In the following we stick to the box constraints for technical reasons.

**Relation to pseudo-boolean optimization.** There is a natural equivalence between MWIS and pseudo-boolean optimization [3]. More precisely, the MWIS problem (1) with non-negative costs  $c$  can be reduced to, e.g., maximization over  $\mathbf{x} \in \{0, 1\}^n$  of the following posiform [3, Thm.4]:

$$\phi(x_1, \dots, x_n) = \sum_{i \in [n]} c_i x_i \cdot \prod_{j: \{i, j\} \in \mathcal{E}} \bar{x}_j. \quad (4)$$

The term *posiform* comes from the non-negativity of the coefficients  $c_i$ .

In the other direction, maximization of an arbitrary posiform  $f(x_1, \dots, x_n) = \sum_{i=1}^p c_i T_i + c_0$ , where  $c_i \geq 0$ ,  $i \in \{0, \dots, p\}$ , and  $T_i = \prod_{j \in A_i} x_j \prod_{k \in B_i} \bar{x}_k$  with  $A_i, B_i \subseteq [n]$  and  $A_i \cap B_i = \emptyset$ , is reducible to MWIS defined over the so called *conflict graph* [3, Thm. 3].

It is known that any pseudo-boolean function can be represented as a posiform up to a constant [3, Prop. 1]. Also, setting all negative costs in (1) to zero preserves the optimal value and may only enlarge the set of optimal solutions. This implies equivalence of MWIS and pseudo-boolean optimization and allows for cross-application of optimization techniques from both domains.

A special case of this relation is a reduction of MWIS (1) by considering a sufficiently large  $M > 0$ <sup>5</sup>

<sup>4</sup>The respective ILP formulation is a special case of the *weighted set partitioning* problem.

<sup>5</sup>It is sufficient to consider  $M > \max_{i \in \mathcal{V}} c_i$ .

to the maximization of the *quadratic* pseudo-boolean function

$$\sum_{i=1}^n c_i x_i - M \cdot \sum_{\{i, j\} \in \mathcal{E}} x_i x_j. \quad (5)$$

The latter, in turn, has a one-to-one correspondence to the *binary pairwise discrete energy minimization problem* [33, Ch. 12]. The respective *local polytope* relaxation [33, Ch. 4] is equivalent to the edge relaxation [32]. Some MWIS algorithms therefore adopt techniques from the field of discrete graphical models [32, 37], however, their guaranteed performance does not go beyond the edge relaxation.

We use the transformation (5) in Section 9 for a primal heuristic supplementing our dual method.

**Solvability and approximation.** The MWIS problem is polynomially solvable for perfect graphs [13]. In particular, this applies to bipartite graphs mentioned above. Efficient methods also exist for other graph families, see [36, Ch. 64.9a] for an overview. Contrary to the closely related vertex cover problem, there are no constant factor approximation algorithms for MWIS [40]. A number of approximation bounds has been obtained for the general problem as well as for its special cases [16, 25], especially wrt. to the maximum degree of the underlying graph [17]. These algorithms often make use of the persistency property of the edge relaxation.

**Primal heuristics** is a popular class of algorithms addressing MWIS, see e.g., [7, 5, 24, 29] and references therein. Apart from the direct application, they can be used in combination with the relaxation-based methods, as in [7] and this work, or, e.g., within reduction-based methods [21]. We get back to the first case in Section 9 and empirically compare to algorithms of both types in Section 10.

**Relation to linear assignment.** The MWIS problem (2) can be seen as a generalization of the *incomplete* linear assignment problem [6], as the ILP formulation of the latter

$$\begin{aligned} \max_{\mathbf{x} \in \{0,1\}^{n \times n}} & \langle \mathbf{c}, \mathbf{x} \rangle \\ \text{s.t. } & \sum_{i \in [n]} x_{ij} \leq 1, j \in [n], \\ & \sum_{j \in [n]} x_{ij} \leq 1, i \in [n]. \end{aligned} \quad (6)$$

is a special case of (2). Incomplete linear assignment is tightly related and reducible to the (complete) linear assignment problem [6, 15] in linear time. From the other viewpoint, linear assignment is a specialization of the optimal transport problem. These facts are important, as the Sinkhorn algorithm and its variants [26] have shown their remarkable efficiency and scalability for the

optimal transport problems. The Sinkhorn algorithm itself [38] is a special case of the famous Bregman method for linear programs [4], which is one of the widely considered entropy optimization techniques [10]. This leads us to the main contribution of our work formulated below.

### 3 Contribution and paper content

We propose a scalable iterative algorithm for the clique cover family of relaxations (3). The algorithm is based on the Bregman method and, therefore, is essentially a smoothed dual coordinate minimization. Our method can be also seen as a generalization of the Sinkhorn algorithm for optimal transport. We propose several variations of our method, with different numerics, scheduling of the smoothing level and sparsity-based speed-up. As a dual method, it operates over the feasible set of the dual problem, but the respective primal variables remain infeasible upon convergence. We propose an efficient method to *project* them to the feasible set of the primal relaxed problem. This leads to feasible primal estimates of the relaxed solution and, as a result, to estimates of the duality gap. In turn, the duality gap estimate results in a new smoothing scheduling method that consistently outperforms the standard feasibility-based scheduling in our experiments.

Convergence of our algorithms follows from those of the Bregman method. Empirically, it is able to attain high quality approximations of the relaxed problem. On large-scale ( $> 100\,000$  graph edges) instances it is notably faster than simplex or interior point methods.

We combine the dual algorithm with a simple but efficient primal heuristic to address the non-relaxed MWIS problem. In our experimental evaluation we were able to find good approximate solutions for large-scale problem instances significantly faster than off the shelf Gurobi ILP solver [14] as well as the reduction-based methods and related primal heuristics [21].

Our code is publicly available on GitHub<sup>6</sup>.

**Paper content.** We analyze the clique cover relaxation (3) and its Lagrange dual in Section 4. We start with a simple coordinate minimization method addressing this problem. Although being a natural baseline, it does not guarantee convergence to the dual optimum as we show.

We introduce the Bregman method and its specialization to the MWIS problem in Section 5. In essence, this method can be seen as a smoothed variant of the above mentioned coordinate minimization algorithm. The larger the smoothing value, controlled by the *temperature* parameter, the faster is the convergence but worse the approximation of the original problem.

<sup>6</sup> <https://github.com/vislearn/libmpopt>

Section 6 describes two numerically stable implementations of the introduced Bregman method specialization. These are essentially the same as used with this type of algorithms for optimal transport problems.

Section 7 considers two strategies of smoothing scheduling. Additionally, a projection method to the feasible set that allows us to obtain feasible primal estimates for the relaxed problem is described here.

Section 8 proposes two sparsity-based strategies to speed-up our dual algorithms. Whereas the first strategy is a heuristic, the second is based on upper-bounding of the possible perturbation of the smoothed dual objective value.

In Section 9, we describe a simple primal heuristic to reconstruct integer solutions of the non-relaxed MWIS problem. Though by itself, it is inferior to other similar methods, in combination with our dual algorithm it shows competitive results.

Finally, Section 10 is devoted to the experimental evaluation. Here we consider two benchmarks, related to image segmentation [27] and vehicle routing [8] respectively. Additionally to the experimental study of different variants of our method, we compare it to the Gurobi general purpose LP and ILP solvers and state-of-the-art reduction-based algorithms and primal heuristics [21, 18, 7, 24].

### 4 Dual of the clique cover relaxation

**Dual problem.** First, we introduce the constraint sets  $J_i = \{j \in [m] : \bar{K}_j \ni i\}$  as the set of cliques containing the variable  $x_i$ . In particular, for any slack variable  $x_{n+j}$  it holds  $J_{n+j} = \{j\}$ .

By dualizing the equality constraints of the clique cover relaxation (3) we obtain its Lagrange dual problem:

$$\begin{aligned} & \min_{\lambda \in \mathbb{R}^m} \left[ \max_{\mathbf{x} \in [0,1]^{n+m}} \langle \mathbf{c}, \mathbf{x} \rangle - \sum_{j=1}^m \lambda_j \left( \sum_{i \in \bar{K}_j} x_i - 1 \right) \right] \\ &= \min_{\lambda \in \mathbb{R}^m} \underbrace{\left[ \sum_{j=1}^m \lambda_j + \max_{\mathbf{x} \in [0,1]^{n+m}} \langle \mathbf{c}^\lambda, \mathbf{x} \rangle \right]}_{D(\lambda)} \end{aligned} \quad (7)$$

where  $\lambda$  are dual variables and  $\mathbf{c}_i^\lambda = c_i - \sum_{j \in J_i} \lambda_j$  are the *reduced* or *reparametrized* costs. From the first line in (7) it follows that  $\langle \mathbf{c}, \mathbf{x} \rangle = \langle \mathbf{c}^\lambda, \mathbf{x} \rangle + \sum_{j=1}^m \lambda_j$  holds for any  $\mathbf{x}$  that satisfies the clique constraints in (3). In other words, the costs of all feasible solutions (that includes integral solutions) of the problem (3), are shifted by the constant  $\sum_{j=1}^m \lambda_j$  with the transformation  $\mathbf{c} \rightarrow \mathbf{c}^\lambda$ . In particular, it implies that the set of optimal solutions of these problems is invariant with respect to this transformation. The latter is sometimes called *equivalent transformation* in the literature therefore.

**Algorithm 1:** Dual coordinate descent algorithm.

---

```

1 while stopping criterion not fulfilled do
2   // loop over cliques:
3   for  $j \in [m]$  do
4     // turn the max. cost in the clique to 0:
5     // pick the clique-largest reduced cost:
6      $i^* \in \arg \max_{i \in \bar{K}_j} c_i^\lambda$ 
7     // ... and make it zero
8      $\lambda_j = \lambda_j + c_{i^*}^\lambda$ 

```

---

**Result:**  $\lambda$ 


---

The dual objective  $D(\lambda)$  is convex piece-wise affine as a maximum of a finite number of affine functions, since  $\max_{\mathbf{x} \in [0,1]^{n+m}} \langle \mathbf{c}^\lambda, \mathbf{x} \rangle = \max_{\mathbf{x} \in \{0,1\}^{n+m}} \langle \mathbf{c}^\lambda, \mathbf{x} \rangle$  in (7). By strong duality the minimum of the dual problem (7) coincides with the maximum of the clique relaxation (3).

Introduce the set  $\text{Sign}(\mathbf{c}) := \arg \max_{\mathbf{x} \in [0,1]^{n+m}} \langle \mathbf{c}, \mathbf{x} \rangle$ . In other words,  $\mathbf{x} \in \text{Sign}(\mathbf{c})$  if

$$x_i = \begin{cases} 0, & \text{if } c_i < 0, \\ 1, & \text{if } c_i > 0, \\ \in [0,1], & \text{if } c_i = 0. \end{cases} \quad (8)$$

The dual value is therefore equal to  $D(\lambda) = \sum_{j=1}^m \lambda_j + \langle \mathbf{c}^\lambda, \mathbf{x}^* \rangle$  for any  $\mathbf{x}^* \in \text{Sign}(\mathbf{c}^\lambda)$ . Different subgradients of  $D$  can be obtained for different values of  $\mathbf{x}^*$  as

$$\frac{\partial D}{\partial \lambda_j}[\mathbf{x}^*] = 1 + \frac{\partial \langle \mathbf{c}^\lambda, \mathbf{x}^* \rangle}{\partial \lambda_j} = 1 + \left\langle \frac{\partial \mathbf{c}^\lambda}{\partial \lambda_j}, \mathbf{x}^* \right\rangle = 1 - \sum_{i \in \bar{K}_j} x_i^*. \quad (9)$$

The last term counts the number of non-zero coordinates of  $\mathbf{x}^*$  in the constraint  $\bar{K}_j$ . The considered subgradient coordinate  $\frac{\partial D}{\partial \lambda_j}[\mathbf{x}^*]$  is equal to 0 if their sum is equal to 1. In other words,  $\lambda$  is dual optimal if and only if  $\text{Sign}(\mathbf{c}^\lambda)$  contains at least one vector feasible for (3). This vector is a solution of the relaxed primal problem:

**Proposition 4.** Let  $\mathbf{x}^* \in \text{Sign}(\mathbf{c}^\lambda)$  and  $\frac{\partial D}{\partial \lambda_j}[\mathbf{x}^*] = 0$  for all  $j \in [m]$ . Then  $\mathbf{x}^*$  is the solution of the respective clique relaxation (3). If additionally  $\mathbf{x}^* \in \{0,1\}^{n+m}$ , then its first  $n$  coordinates constitute a solution of the non-relaxed problem (2).

**The dual coordinate minimization Algorithm 1** iteratively considers each clique and changes the value of the respective dual variable. This is done such that the largest reduced cost of the nodes belonging to the clique becomes zero.

Being very simple, this algorithm implements the *coordinate minimization* principle. Indeed, the dual objective  $D$  is convex. Therefore, its restriction to the  $j$ -th variable  $\lambda_j$  is convex as well. In turn, a necessary and

sufficient optimality condition for the restricted convex function is existence of a zero subgradient. In this case, after each inner iteration of Algorithm 1 there should exist  $\mathbf{x}^* \in \text{Sign}(\mathbf{c}^\lambda)$  such that  $\frac{\partial D}{\partial \lambda_j} = 1 - \sum_{i \in \bar{K}_j} x_i^* = 0$  (see (9)) for the value of  $j$  being an index of the currently processed clique. To obtain such  $\mathbf{x}^*$  it is sufficient to set  $x_{i^*}^* = 1$  and  $x_i^* = 0$  for  $i \in \bar{K}_j \setminus \{i^*\}$ , where  $i^*$  is defined as in Algorithm 1.

Unfortunately, coordinate minimization is not guaranteed to converge to the optimum for convex piece-wise affine functions [2, Ch. 2.7]. This holds in general, as well as for the dual (7) in particular, as shown by the following example:

**Example 1.** Consider an MWIS problem in format (3) with the following  $m = 6$  constraints:

$$x_1 + x_2 + x_6 = 1 \quad (10)$$

$$x_2 + x_3 + x_7 = 1 \quad (11)$$

$$x_3 + x_1 + x_8 = 1 \quad (12)$$

$$x_1 + x_3 + x_4 + x_9 = 1 \quad (13)$$

$$x_4 + x_5 + x_{10} = 1 \quad (14)$$

$$x_5 + x_3 + x_{11} = 1 \quad (15)$$

The coordinates with indices 6 and above correspond to the slack variables and can be found in a single equation only. We also assume  $c_i^\lambda = 0$  for  $i \in [5]$  and  $c_i^\lambda < 0$  for  $i > 5$ .

Obviously this  $\lambda$  is a fix-point of Algorithm 1. We will show that this point is not optimal. For this, it is sufficient to show that the set  $\text{Sign}(\mathbf{c}^\lambda)$  does not contain feasible vectors. Assume it does and  $\mathbf{x} \in \text{Sign}(\mathbf{c}^\lambda)$ , then  $x_i = 0$  for  $i > 5$  as  $c_i^\lambda < 0$ . Assume  $x_1 = \gamma \geq 0$ . This implies  $x_2 = 1 - \gamma$ , and  $x_3 = \gamma = 1 - \gamma = 0.5$  and hence  $x_1 = x_2 = x_3 = 0.5$  from the first three constraints. The next two constraints imply  $x_4 = 0$  and  $x_5 = 1$ . The last equality does not hold as  $x_5 + x_3 = 1.5 > 1$ , which is a contradiction.

Unfortunately, the fix-points attained by Algorithm 1 in our experiments give only a loose approximation of the dual optimum, although the obtained lower bound is usually much better than those of the edge relaxation, see Figure 1(a) in Section 10. Therefore, Algorithm 1 can only be seen as a weak baseline. However, it is very important due to the fact that the convergent algorithms we consider below are its smoothed modifications.

## 5 Bregman method for MWIS

The Bregman method [4] can be used to address linear programs  $\{\max_{\mathbf{x} \geq 0} \langle \mathbf{c}, \mathbf{x} \rangle, \text{ s.t. } A\mathbf{x} = \mathbf{b}\}$  through solving their approximations  $\{\max_{\mathbf{x} \geq 0} \langle \mathbf{c}, \mathbf{x} \rangle + T\mathcal{H}(\mathbf{x}), \text{ s.t. } A\mathbf{x} = \mathbf{b}\}$  with the function  $\mathcal{H}$  being differentiable and strictly concave on  $\mathbf{x} \geq 0$ .<sup>7</sup> Parameter  $T > 0$  is the *temperature*

<sup>7</sup>In general the function  $\mathcal{H}(\mathbf{x})$  must be differentiable and strictly concave on a closed convex set  $S$ . The latter must include the feasible set  $\{\mathbf{x} \geq 0: A\mathbf{x} = \mathbf{b}\}$  of the problem as well as the unconstrained optimum of its objective  $\langle \mathbf{c}, \mathbf{x} \rangle + T\mathcal{H}(\mathbf{x})$ , that must belong to the interior of  $S$ , see [4] for details.

---

**Algorithm 2:** Naive Bregman method for MWIS.

---

**Input:**  $x_i = \exp(c_i/T)$ ,  $i \in [n+m]$

1 **while** stopping criterion not fulfilled **do**

// loop over cliques:

2 **for**  $j \in [m]$  **do**

// make the sum of  $x_i$  within the clique = 1

3  $s := \sum_{i \in \bar{K}_j} x_i$

4  $x_i := \frac{x_i}{s}$ ,  $\forall i \in \bar{K}_j$

---

**Result:**  $\mathbf{x}$

---

or *smoothing* parameter that regulates the trade-off between approximation accuracy and convergence speed. The latter problem takes the form of the *smoothed clique cover relaxation* in our case:

$$\begin{aligned} & \max_{\mathbf{x} \in [0,1]^{n+m}} \langle \mathbf{c}, \mathbf{x} \rangle + T\mathcal{H}(\mathbf{x}) \\ & \text{s.t. } \sum_{i \in \bar{K}_j} x_i = 1, j \in [m], \end{aligned} \quad (16)$$

since the box constraints  $\mathbf{x} \in [0,1]^{n+m}$  in (16) are equivalent to  $\mathbf{x} \geq \mathbf{0}$  as noted in Remark 1.

In our application, as well as in the optimal transport literature [26], the function  $\mathcal{H}$  is defined as  $\mathcal{H}(\mathbf{x}) := -\sum_{i=1}^{n+m} (x_i \log x_i - x_i)$ , i.e.,  $\mathcal{H}$  is the entropy shifted by a linear function. The latter is used for the sake of resulting formulas.

On each iteration of the Bregman method the current iterate  $\mathbf{x}$  is projected to the hyperplane determined by a single row of the constraint matrix  $A$ . In case of the function  $\mathcal{H}$  defined as above and constraints of the form  $\sum_{i \in \bar{K}_j} x_i = 1$  as in (16), this projection results in *normalization* of the respective coordinates of  $\mathbf{x}$ , as given by Algorithm 2. The only computation that depends on the cost vector  $\mathbf{c}$  is the initialization of the algorithm: Whereas it converges to a feasible point for *arbitrary* initialization  $\mathbf{x} > \mathbf{0}$ , its limit point is a solution to the problem (16) only if properly initialized. When applied to the linear assignment problem Algorithm 2 is usually referred to as *Sinkhorn algorithm* due to the seminal paper [38] showing that iterative normalization of a square matrix turns it into a bi-stochastic one.

The following statements formalize the main properties of Algorithm 2:

**Lemma 1.** *After the first outer iteration of Algorithm 2 it holds  $\mathbf{0} \leq \mathbf{x} \leq \mathbf{1}$ .*

**Proposition 5.** *Iterates of Algorithm 2 converge to the solution of the smoothed clique cover relaxation (16).*

To be able to apply Algorithm 2 to the clique relaxation (3) one has to define *how to select the temperature T* as well as *how to deal with situations when  $s = \sum_{i \in \bar{K}_j} x_i$  is numerically equal to zero*. The latter may happen due to computation of  $x_i = \exp(c_i/T)$  for low temperatures

---

**Algorithm 3:** Bregman method in log domain.

---

1 **while** stopping criterion not fulfilled **do**

// loop over cliques:

2 **for**  $j \in [m]$  **do**

// make the largest cost in the clique  $\approx 0$

3  $i^* \in \arg \max_{i \in \bar{K}_j} c_i^\lambda$

4  $\lambda_j := \lambda_j + c_{i^*}^\lambda + T \log \sum_{i \in \bar{K}_j} \exp \frac{c_i^\lambda - c_{i^*}^\lambda}{T}$

---

**Result:**  $\lambda$

---

and negative costs, and triggers an error during division to  $s$ . We cover the second question first in Section 6 and get back to the first one in Section 7.

## 6 Numerics

**Log-domain numerics.** Consider Algorithm 3. Note that it differs from Algorithm 1 by the single term  $T \log \sum_{i \in \bar{K}_j} \exp \frac{c_i^\lambda - c_{i^*}^\lambda}{T}$  in the computation pipeline. The following presentation recapitulates the well-known result for this type of algorithms in the optimal transport domain:

**Lemma 2.** *Algorithm 3 is equivalent to Algorithm 2 through the transformation  $\mathbf{x} = \exp(\mathbf{c}^\lambda/T)$ .*

Contrary to Algorithm 2, Algorithm 3 is numerically stable. Its stability follows from  $c_i^\lambda - c_{i^*}^\lambda \leq 0$  and, therefore,  $\exp \frac{c_i^\lambda - c_{i^*}^\lambda}{T} \in (0, 1]$ , and  $c_{i^*}^\lambda - c_{i^*}^\lambda = 0$  implying  $\sum_{i \in \bar{K}_j} \exp \frac{c_i^\lambda - c_{i^*}^\lambda}{T} > 1$ . The latter is sufficient to have a numerically stable logarithm computation.

**Lemma 3.** *After the first iteration of Algorithm 3 the reduced costs  $\mathbf{c}^\lambda$  remain non-positive, e.g.,  $\mathbf{c}^\lambda \leq \mathbf{0}$ .*

**Proposition 6.** *Algorithm 3 converges to the optimum of the dual smoothed clique cover relaxation problem*

$$\min_{\lambda} D^T(\lambda) := \sum_{j=1}^m \lambda_j + \max_{\mathbf{x} \in [0,1]^{n+m}} \left( \langle \mathbf{c}^\lambda, \mathbf{x} \rangle + T\mathcal{H}(\mathbf{x}) \right), \quad (17)$$

and implements the coordinate minimization principle. In particular,  $D^T$  is convex differentiable and right after processing the clique  $j \in [m]$  in Line 4 it holds  $\frac{\partial D^T}{\partial \lambda_j} = 0$ .

Propositions 5–6 imply that the dual iterates  $\lambda$  of Algorithm 3 determine the primal ones  $\mathbf{x} = \exp(\mathbf{c}^\lambda/T)$  and the latter converge to the solution of the smoothed clique relaxation (16).

Along with the advantages such as numerical stability and possibility to estimate an upper bound due to the explicit computations of the dual iterates, Algorithm 3 has a major disadvantage: It has high computational cost due to extensive exponentiations. An alternative way to perform computations that allows to keep advantages of Algorithm 3 and avoid its disadvantages is reviewed in the following paragraph.

**Exp-domain numerics with stabilization** is represented by Algorithm 4. It keeps track of the exponentiated version  $\alpha_j = \exp(-\lambda_j/T)$ ,  $j \in [m]$ , of the dual variables. Note that for any  $j \in [m]$  and any  $i \in \bar{K}_j$ , it holds

$$\begin{aligned} x_i &= \exp(c_i^\lambda/T) = \exp\left(\left(c_i - \sum_{j' \in J_i} \lambda_{j'}\right)/T\right) \\ &= \exp\left(\left(c_i - \sum_{j' \in J_i \setminus \{j\}} \lambda_{j'}\right)/T\right) \cdot \exp(-\lambda_j/T) \\ &= \exp\left(\left(c_i - \sum_{j' \in J_i \setminus \{j\}} \lambda_{j'}\right)/T\right) \cdot \alpha_j \quad (18) \end{aligned}$$

So  $x_i$ ,  $i \in \bar{K}_j$ , are proportional to  $\alpha_j$ . Hence, instead of normalizing  $x_i$ , we can update  $\alpha_j$  by diving it by the normalization factor  $s$ , see Line 4. The main advantage of this approach is an explicit computation of the dual variables (up to the logarithm operation). Since computation of the normalizing factor  $s$  requires values of  $\mathbf{x}$ , we update  $\mathbf{x}$  directly as well, see Line 6.

As long as  $\alpha$  remains close enough to 1 (Line 5, see Section 10 for the used values of the *stabilization threshold*  $\tau_{\text{stab}}$ ), this implies stable computations for  $\alpha$  and  $\mathbf{x}$  (Lines 4, 6). Should  $\alpha$  become very large or very small (Line 5), the computations may get imprecise and, therefore, one switches to the expensive computations in the log-domain to stabilize them (Lines 8–11).

Note, however, that close to the optimum of the smoothed problem (16), and, therefore, feasibility of  $\mathbf{x}$ , computations in Algorithm 4 *do not require stabilization* as  $s \approx 1$  and, hence,  $\alpha \approx 1$  in this case. This emphasizes importance of the proper selection or scheduling of the temperature parameter  $T$  as the latter influences the distance to the non-smoothed optimum of the current primal-dual pair  $(\mathbf{x}, \lambda)$ . We consider this question in Section 7.

## 7 Smoothing scheduling

The lower the temperature  $T$  is, the better the smoothed clique cover relaxation (16) approximates its non-smoothed counterpart (3), see [41]. Given a required approximation level, one could imagine two strategies of temperature selection. The first one is the *fixed* temperature. Although being very simple, it leads to very slow algorithms. First, because the Bregman algorithm makes only small progress for low temperatures. Second, because the numerical stabilization in Algorithm 4 can be required very often for computations far from the optimum. This would eliminate the speed advantage of the exp-domain-based Algorithm 4 over the log-domain-based Algorithm 3.

Hence, a practical solution is the *temperature scheduling*, i.e., starting with a high value of  $T$  and decreasing it

**Algorithm 4:** Stabilized Bregman method in exp-domain.

---

**Input:**  $\alpha_j = 1$ ,  $j \in [m]$ ;  $x_i = \exp(c_i^\lambda/T)$ ,  $i \in [n]$

- 1 **while** stopping criterion not fulfilled **do**
- 2   **for**  $j \in [m]$  **do**
- 3     // Compute sum over the clique
- 4      $s := \sum_{i \in \bar{K}_j} x_i$
- 5     // update exponentiated dual
- 6      $\alpha_j := \alpha_j/s$
- 7     **if**  $\alpha_j + 1/\alpha_j < \tau_{\text{stab}}$  **then**
- 8       // if  $\alpha_j \approx 1$  run naive Bregman method
- 9        $x_i := x_i/s$
- 10     **else**
- 11       // stabilize:
- 12       // push  $\alpha$  into  $\lambda$  to obtain a dual
- 13       solution
- 14       **for**  $j \in [m]$  **do**
- 15          $\lambda_j := \lambda_j - T \log \alpha_j$
- 16        $\alpha_j := 1$  // reinitialize  $\alpha$
- 17       // update  $x$  in a stable way
- 18        $x_i := \exp(c_i^\lambda/T)$ ,  $i \in \bar{K}_j$

// push  $\alpha$  into  $\lambda$  to obtain a dual solution

**for**  $j \in [m]$  **do**

$\lambda_j := \lambda_j - T \log \alpha_j$

**Result:**  $(\mathbf{x}, \lambda)$

---

as the computation progresses. We consider two methods for the temperature scheduling below.

### 7.1 Method 1: Feasibility-based

Feasibility constraints satisfaction is the standard stopping criterion in the optimal transport literature [35], used to decide whether it is time to decrease the temperature. Typically, one checks whether

$$\left| \sum_{i \in \bar{K}_j} x_i - 1 \right| \leq \tau_{\text{feas}}, \forall j \in [m], \quad (19)$$

for some predefined *feasibility threshold*  $\tau_{\text{feas}} \geq 0$ . Should the constraints (19) be fulfilled, one drops the temperature by the predefined factor  $0 < \tau_{\text{drop}} < 1$ , i.e.  $T := \tau_{\text{drop}} T$ . For higher efficiency the conditions (19) are checked only each  $\tau_{\text{batch}} \in \mathbb{N}$  iterations.

**Remark 2.** To simplify selection of the initial temperature and keep computations numerically stable we

- run a single iteration of Algorithm 1 to get  $\mathbf{c}^\lambda < 0$ , and
- scale all costs such that they lie in the interval  $[-1, 0]$ .

After these operations we launch Algorithm 4 with the initial temperature  $T = 0.01$ .

**Remark 3.** There is an alternative method for feasibility-based temperature scheduling, introduced in [20] for the quadratic assignment problem and equivalent to the above rule with  $\tau_{\text{drop}} = 0.5$ . Although authors report its numerical stability in their experiments, for other problem instances it may require stabilization exactly as Algorithm 4 does.

## 7.2 Method 2: Duality gap-based

Duality gap is an alternative way to control the distance to the optimum when dual variables  $\lambda$  are computed explicitly, i.e., in Algorithm 3 or 4. Let  $\hat{\mathbf{x}}$  and  $\mathbf{x}^*$  be a feasible and an optimal solutions to the smoothed clique cover relaxation (16) respectively. Let also  $\lambda$  and  $\lambda^*$  be a feasible and an optimal dual solutions for (17). The strong duality implies  $\langle \mathbf{c}, \hat{\mathbf{x}} \rangle + T\mathcal{H}(\hat{\mathbf{x}}) \leq \langle \mathbf{c}, \mathbf{x}^* \rangle + T\mathcal{H}(\mathbf{x}^*) = D^T(\lambda^*) \leq D^T(\lambda)$ . A progress of the Bregman method is assured if the inequalities above hold strictly, i.e.,  $T < \frac{D^T(\lambda) - \langle \mathbf{c}, \hat{\mathbf{x}} \rangle}{\mathcal{H}(\hat{\mathbf{x}})}$ . This inequality turns into equality in the optimum of the smoothed problems (16)–(17). The respective temperature update condition therefore may look like

$$T > \tau_{\text{gap}} \frac{D^T(\lambda) - \langle \mathbf{c}, \hat{\mathbf{x}} \rangle}{\mathcal{H}(\hat{\mathbf{x}})} \quad (20)$$

for a suitable predefined  $0 < \tau_{\text{gap}} < 1$ .

To ensure monotonicity of the temperature, we update it by setting to

$$T := \min \left\{ T, \tau_{\text{gap}} \frac{D^T(\lambda) - \langle \mathbf{c}, \hat{\mathbf{x}} \rangle}{\mathcal{H}(\hat{\mathbf{x}})} \right\} \quad (21)$$

each  $\tau_{\text{batch}} \in \mathbb{N}$  iterations. Between temperature changes Algorithm 3, as well as Algorithm 4 can be used.

## 7.3 Feasible primal estimates for Method 2

**Obtaining feasible primal estimates.** Let  $C$  stand for the feasible set of (16). Computations (20) and (21) require a feasible  $\hat{\mathbf{x}}$ , i.e.,  $\hat{\mathbf{x}} \in C$ . Contrary to the unconstrained dual iterates  $\lambda$  their primal counterparts  $\mathbf{x} = \exp(\mathbf{c}^\lambda / T)$  are infeasible until convergence, i.e.,  $\mathbf{x} \notin C$ . To obtain feasible iterates we project  $\mathbf{x}$  to the set  $C$ :

**Definition 1.** A mapping  $\mathcal{P}: \mathbb{R}_{\geq 0}^{n+m} \rightarrow C$  is called projection, if it is idempotent, i.e.,  $\mathcal{P}(\mathcal{P}(\mathbf{x})) = \mathcal{P}(\mathbf{x})$ , and continuous. The latter, in particular, guarantees that  $\mathbf{x}^t \xrightarrow{t \rightarrow \infty} \mathbf{y} \in C$  implies  $\mathcal{P}(\mathbf{x}^t) \xrightarrow{t \rightarrow \infty} \mathcal{P}(\mathbf{y}) = \mathbf{y}$ .

Consider Algorithm 5 that introduces what we call a *truncation projection*. The algorithm checks all coordinates of  $\mathbf{x}$  and fixes their values in the projection  $\hat{\mathbf{x}}$  as long as they don't violate the clique constraints. The value is truncated if necessary to avoid constraint violation. The slack variables  $\hat{x}_{n+j}$  are set to guarantee equality in the clique constraints.

Algorithm 5 has the following properties:

---

### Algorithm 5: Truncation projection.

---

**Input:**  $\mathbf{x} \in \mathbb{R}_{+}^{n+m}$   
 // Initialize the feasible solution:  
 1  $\hat{\mathbf{x}} := \mathbf{0} \in \mathbb{R}^{n+m}$  // set all coordinates to 0 and  
 // set slack variables to 1 for all  $m$  cliques:  
 2  $\hat{x}_{n+j} = 1, j \in [m]$   
 // Update all non-slack variables:  
 3 **for**  $i \in [n]$  **do**  
 // max. value of  $x_i$  fitting clique constraints:  
 4  $M := \min_{j \in J_i} \hat{x}_{n+j}$   
 5  $\hat{x}_i := \min\{x_i, M\}$  // truncate  $x_i$  if needed  
 6 **for**  $j \in J_i$  **do**  
 7    $\hat{x}_{n+j} := \hat{x}_{n+j} - \hat{x}_i$  // decrease the slacks resp.

**Result:**  $\mathcal{P}(\mathbf{x}) := \hat{\mathbf{x}}$

---

**Lemma 4 (Feasibility).** The vector  $\hat{\mathbf{x}}$  is always feasible at the end of each iteration of the outer loop defined in Line 3.

**Lemma 5 (Idempotence).** If the input  $\mathbf{x}$  is feasible, then  $\mathcal{P}(\mathbf{x}) = \mathbf{x}$ .

**Lemma 6 (Continuity).** The mapping  $\mathcal{P}: \mathbb{R}_{\geq 0}^{n+m} \rightarrow C$  is continuous. Moreover,

$$\left| \sum_{i \in \bar{K}_j} x_i - 1 \right| \leq \epsilon, \forall j \in [m]. \quad (22)$$

implies

$$|x_i - \mathcal{P}(x)_i| \leq \epsilon, \quad \forall i \in [n]. \quad (23)$$

Lemmas 4–6 trivially result in

**Theorem 1.** Mapping  $\mathcal{P}(\mathbf{x})$  defined by Algorithm 5 is a projection to the feasible set  $C$ .

## 8 Sparsity-based speedup

As the temperature gets lower, the majority of values of the primal solution  $\mathbf{x} = \exp(\mathbf{c}^\lambda / T)$  get closer to zero exponentially fast. Their influence on the value of the sum of all variables in a given clique  $s := \sum_{i \in \bar{K}_j} x_i$ , see Line 3 in Algorithm 4, reduces accordingly. Respectively, most of them can be completely ignored during computation to speed-up the latter. Below we consider two methods making use of this observation.

**Heuristic truncation.** In our first method we excluded from the summation all variables in a given clique if their values were at least a factor  $10^{-8}$  smaller than the largest element in the clique. This reduced the efficient size of the cliques up to 10 times leading to significant speedup.

However, such a heuristic speedup may lead to an uncontrolled increase of the smoothed dual value  $D^T$

ruining algorithms convergence. This behavior is well-known in the optimal transport domain, see [34, Example 3.5]. Hence, below we derive a method that takes this issue into account.

**Truncation based on a bounded dual perturbation (accurate truncation).** Similarly to [35], our *accurate truncation* is based on the stabilization technique that guarantees a limited maximum value of the exponentiated dual variables  $\alpha$ , see Algorithm 4. Contrary to [35], we compute the allowed truncation value based on the recent improvement of the smoothed dual value  $D^T$  instead of the primal-dual gap.

To this end consider the following statement:

**Lemma 7.** *For any  $T \geq 0$  and  $\mathbf{c} \leq 0$  it holds:*

$$\max_{\mathbf{x} \in [0,1]^{n+m}} (\langle \mathbf{c}, \mathbf{x} \rangle + T\mathcal{H}(\mathbf{x})) = T \sum_{i=1}^{n+m} \exp(c_i/T). \quad (24)$$

According to Lemma 7 the dual value  $D^T$  is equal to

$$\begin{aligned} D^T(\boldsymbol{\lambda}) &= \sum_{j=1}^m \lambda_j + T \sum_{i=1}^{n+m} \exp(c_i/T) \prod_{j \in J_i} \exp(-\lambda_j/T) \\ &= \sum_{j=1}^m \lambda_j + T \sum_{i=1}^{n+m} x_i \prod_{j \in J_i} \alpha_j. \end{aligned} \quad (25)$$

Consider the truncated primal estimates

$$\bar{x}_i = \begin{cases} 0, & \text{if } x_i < \epsilon_i, \\ x_i, & \text{otherwise} \end{cases} \quad (26)$$

and the respective smoothed dual value

$$\bar{D}(\boldsymbol{\lambda}) := \sum_{j=1}^m \lambda_j + T \sum_{i=1}^{n+m} \bar{x}_i \prod_{j \in J_i} \alpha_j. \quad (27)$$

Let  $\delta$  be a maximum error in computation of  $D^T$  allowed due to truncation:

$$\begin{aligned} \delta &:= D^T(\boldsymbol{\lambda}) - \bar{D}(\boldsymbol{\lambda}) = T \sum_{i=1}^{n+m} (x_i - \bar{x}_i) \prod_{j \in J_i} \alpha_j \\ &\leq T \sum_{i=1}^{n+m} \epsilon_i \prod_{j \in J_i} \tau_{\text{stab}} = T \sum_{i=1}^{n+m} \epsilon_i \tau_{\text{stab}}^{|J_i|}. \end{aligned} \quad (28)$$

Hence, setting

$$\epsilon_i \leq \frac{\delta}{T(n+m)\tau_{\text{stab}}^{|J_i|}} \quad (29)$$

guarantees that the truncation error in computation of the smoothed dual value does not exceed  $\delta$ . In our experiments we set  $\delta$  to 0.1 of the smoothed dual value improvement attained in the previous computation batch.

**Algorithm 6:** Greedy solution generation.

---

**Input:**  $\mathbf{c}^\lambda \in \mathbb{R}^{n+m}$  // reduced costs

- 1  $\mathbf{x} := -\mathbf{1} \in \mathbb{R}^{n+m}$  // initialize  $\mathbf{x}$  as undefined
- // iterate over all cliques in random order
- 2 **for**  $j \in \text{shuffle}([m])$  **do**
- // skip cliques with set nodes
- 3 **if**  $\{i \in \bar{K}_j \mid x_i = 1\} = \emptyset$  **then**
- | // find assignable & locally optimal node
- 4  $i^* := \arg \max_{i \in \bar{K}_j \text{ s.t. } x_i = -1} c_i^\lambda$
- 5  $x_{i^*} := 1$  // set it to one
- | // and all its graph neighbors to zero:
- 6 **for**  $i: \{i^*, i\} \in \mathcal{E}$  **do**
- | |  $x_i := 0$
- 7

---

**Result:**  $\mathbf{x}$

---

## 9 Simple primal heuristic

Although the primary subject of our work is the dual optimization, we have implemented a simple primal heuristic to be able to compare to existing methods that return solutions of the non-relaxed MWIS problem. Our primal heuristic consists of two iteratively repeating steps: (i) A randomized *greedy feasible solution proposal generation* and (ii) its *optimized recombination* with the best found solution so far.

A similar primal algorithm for the MWIS problem has been proposed, e.g., in [7], with the main difference that a local search step is additionally applied to each generated solution proposal prior to recombination.

**Our greedy proposal generation step** makes use of the dual optimization by being applied to the problem with the reduced costs  $\mathbf{c}^\lambda$  instead of the original ones  $\mathbf{c}$ .

The pseudo-code of the generation step is represented by Algorithm 6. It considers a graph with additional nodes, one per clique, corresponding to the slack variables introduced in (2). The algorithm randomly selects a yet unprocessed clique and adds the node with the lowest cost in the clique to the solution proposal. This node and all adjacent nodes are removed from the graph. The process is repeated until no nodes are left.

**The optimal recombination (also known as crossover or fusion)** step solves the MWIS problem (1) only for those variables whose values *differ* in the best integer solution found so far and in the newly generated solution proposal. The values of all other variables are fixed to the values in best integer solution found so far. It is known [9] that such optimal recombination problem is reducible in linear time to the min-st-cut/max-flow and is efficiently and exactly solvable therefore. Instead, we opted for reducing it to a special form of the quadratic pseudo-boolean maximization problem (see Section 13), which can itself be efficiently solved via min-st-cut. This alternative approach was used since

dataset	# instances	# nodes	# edges	# cliques	avg. clique size
AVR-large	17	127 k – 882 k	43 M – 344 M	5.4 k – 38 k	120.2
AVR-medium	16	10 k – 84 k	126 k – 39 M	1.8 k – 48 k	24.4
AVR-small	5	979 – 14 k	2.4 k – 44 k	805 – 15 k	3.2
MSCD	21	5 k – 8 k	66 k – 198 k	22 k – 36 k	8.8

**Table 1:** Datasets used for evaluation. We split the AVR dataset into AVR-small, AVR-medium and AVR-large based on the number of nodes. Here **# nodes** and **# edges** stand for the number of nodes and edges in the graph representation of the problem respectively, **# cliques** gives the number of clique constraints in the respective ILP representation (2), and **avg. clique size** is the average clique size per instance averaged over the number of instances in the dataset.

our implementation relies on software [31] that requires the quadratic pseudo-boolean function as input.

**Related work on proposal generation** Algorithm 6 resembles the WG algorithm of [17, Thm. 3] that works with non-negative costs. Let  $\delta_i$  be the node degree. The WG algorithm iteratively and greedily adds to the solution the node  $i^* = \arg \max_{i \in V} c_i / \delta_i$  and removes it and its neighbors from the graph. Hence, node degrees change on each step of the algorithm, and one has to maintain a priority queue, that slows down the algorithm. To speed up computations, this generation method is used to generate only the very first feasible solution proposal in [7]. For further solution proposals the changes in the node degrees during generation are not taken into account.

Our proposal generation is much faster than the WG algorithm, since we do not take the node degrees and their respective changes into account. Importantly, as the dual iterates  $\lambda$  get closer to the dual optimum, our algorithm becomes closer to the WG algorithm. This is because the optimal cost within each clique gets nearly zero (cf. Algorithm 3), just like its weighted degree  $c_i / \delta_i$ .

## 9.1 Discussion: Usage of the relaxed solution.

As mentioned above, our primal heuristic profits from the relaxation optimization by employing the reduced costs  $\mathbf{c}^\lambda$  instead of the original ones  $\mathbf{c}$ . The work [7] instead uses the relaxed primal solution  $\mathbf{x} \in [0, 1]^n$  in the local search procedure by arguing that “*a node with a high value in the relaxed solution is more likely to be part of a good solution to the MWIS*”. This argument, however, has no theoretical support for the clique cover relaxation. As follows from Proposition 4, *all* non-zero fractional-valued coordinates of the optimal primal solution  $\mathbf{x}$  correspond to *zero* reduced costs.<sup>8</sup> And the other way around: Nodes those reduced costs are lower than zero correspond to *zero*-valued coordinates of the

<sup>8</sup>In fact, in multiple duality-based algorithms such as ours or, e.g., the primal simplex algorithm, the optimal reduced costs are non-positive. So, *all* non-zero coordinates of  $\mathbf{x}$  correspond to *zero*-valued reduced costs.

optimal primal relaxed solution, independently on the actual cost values. Therefore, we argue that these are the reduced costs that contain essential information about LP relaxation that can be used in primal heuristics and not the primal relaxed solutions themselves. Although authors of [7] report improvement of their local search due to usage of the primal LP solution, we suspect that the main information which turns to be useful for their algorithm, is distinguishing between zero and non-zero primal LP values, and, respectively, zero- and non-zero reduced costs. Yet, should the usage of the primal relaxed solutions be preferable for any reason, our truncation projection Algorithm 5 provides their estimates even before the dual algorithm reaches the optimum.

Unfortunately, in case of the MWIS problem, usage of the reduced costs has also disadvantages. That is, our reduced costs describe the modified problem (3), which constitutes a special case of the *set partitioning* problem. Although many primal heuristics can be adjusted to cope with this modification, this adjustment is critical for them to function properly. For example, reduced costs are non-positive and any sensible MWIS algorithm ignores nodes with non-positive costs as there is always an optimal solution consisting of nodes with positive costs only.

## 10 Experimental evaluation

**Datasets.** In our evaluation we focus on large, real-world MWIS problems. This is in contrast to prior studies that predominantly utilized augmented unweighted instances with artificial randomized weights (cf. [21]). Not only the variability in random weights among these studies makes direct comparisons difficult, but the random weights themselves raise the question of the results generalization in real-world applied scenarios. Moreover, even usage of existing non-randomly weighted graphs as a test bed for the algorithms (cf. [12]) raises the question of practical usefulness, unless finding MWIS on these graphs has a specific value for some application.

All datasets we consider are readily represented as clique graphs, so we reuse these cliques in our algorithms.

*Amazon Vehicle Routing* [8]. These instances are derived from real-world long-haul vehicle routing problems at Amazon [1]. This dataset contains by far the largest MWIS instances which are publicly available, see Table 1. In each of the problems the nodes describe a set of routes and the cliques describe conflicts between them based on shared drivers or loads. We split this datasets into three subsets, with small (*AVR-small*), medium (*AVR-medium*) and large (*AVR-large*) problem instances, see Table 1 for details.

*Meta-Segmentation for Cell Detection (MSCD)* This dataset is derived from semi-automated labeling problems for cell segmentations [27, Ch. 7] and has been kindly provided by the author of [27]. We make this real-world MWIS dataset publicly available for usage by other researchers<sup>9</sup>. In each instance the nodes represent segmentations that are generated by multiple algorithms and, therefore, overlap with each other. The MWIS problem consists in selecting their non-overlapping subset with the minimal total cost (maximal total weight). The size of the instances from this datasets lies between *AVR-medium* and *AVR-small*, see Table 1.

**Algorithms.** For the experimental evaluation we use the following our algorithms:

- *dualLP-Algorithm 1* – the non-smoothed dual coordinate descent Algorithm 1.
- *LP-Algorithm 3 (feasibility scheduling)* – the Bregman method in the log-domain with the feasibility-based smoothing scheduling, see Section 7.1;
- *LP-Algorithm 4 (feasibility scheduling)* – the stabilized Bregman method in exp-domain with the feasibility-based smoothing scheduling, see Section 7.1. No sparsity-based speedup is utilized.
- *LP-Algorithm 4 (duality gap scheduling)* – the stabilized Bregman method in exp-domain with the duality gap-based smoothing scheduling, see Section 7.2. No sparsity-based speedup is utilized.
- *LP-Algorithm 4 (duality gap scheduling & heuristic/accurate truncation)* – the stabilized Bregman method in exp-domain with the the duality gap-based smoothing scheduling from Section 7.2, with heuristic or accurate truncation method utilized for sparsity-based speedup, see Section 8.
- *ILP-Algorithm 4 (duality gap scheduling & heuristic/accurate truncation)* – the same as the previous algorithm, but with an additionally computed our primal heuristic from Section 9.

The three methods denoted as *LP-\*\*\** are run in a pure LP mode, without the primal heuristic. The primal bound for them is computed with Algorithm 5. All

<sup>9</sup>See <https://vislearn.github.io/libmpopt/mwis2024/>.

algorithms in the list use the same parameter values, where applicable:  $\tau_{\text{batch}} = 50$ ,  $\tau_{\text{drop}} = 0.5$ ,  $\tau_{\text{feas}} = 0.01$ ,  $\tau_{\text{gap}} = 0.5$ , starting temperature  $T = 0.01$ . All algorithms but those that utilize *accurate speedup* use  $\tau_{\text{stab}} = 10^{30}$ , otherwise  $\tau_{\text{stab}} = 10$  to allow for an efficient truncation according to (29).

We compare them to the following competing methods:

- *LP-Gurobi simplex/barrier* – Gurobi optimizer [14] in single-threaded LP mode with simplex or barrier method respectively. The problem formulation corresponds to the LP relaxation of the clique cover formulation (2). We lowered the optimality gap setting to zero to not let Gurobi exit prematurely. Apart from that the default parameters are used.
- *ILP-Gurobi barrier* – Gurobi optimizer [14] in single-threaded ILP mode with the barrier method used to compute the basic relaxation respectively. The barrier method is chosen as it leads to faster results for large problem instances. The addressed ILP problem is (2).
- *KaMIS branch & reduce / reduce & local-search* – Authors of the KaMIS framework [21] claim their state-of-the-art performance on large-scale MWIS problem instances, therefore we selected them as a representative of dedicated optimization techniques. The framework addresses MWIS problems with reduction rules and branching on variables (*branch & reduce*), or by running a local search method after an initial reduction (*reduce & local-search*). Both variants are used with default parameters.
- *KaMIS local-search only* – a representative of the local search paradigm for MWIS solvers. We obtained it by disabling the reduction code.
- *METAMIS* [7], *METAMIS+LP* [7], *ILSVND* [24] – recent primal MWIS heuristics. In contrast to other algorithms, we did not execute these methods ourselves, but compared to the results presented in [7].

All experiments were run on an Intel Core i7-4770 CPU (3.40GHz) with wall-clock time measurements. To reduce the influence of background processes we run each experiment 6 times and report the best run.

**Ablation study for the LP relaxation (Figure 1(a)).** Here we compare all our *LP-Algorithm \*\*\** algorithms against each other on the *AVR-medium* dataset. To this end, we provide primal-dual convergence plots averaged over all instances in the dataset. Due to similarity of the instances the averaged plot looks qualitatively similar to individual plots for each problem instance within dataset. Analogous averaged plots for other datasets look qualitatively similar to Figure 1(a), therefore we omit them here.

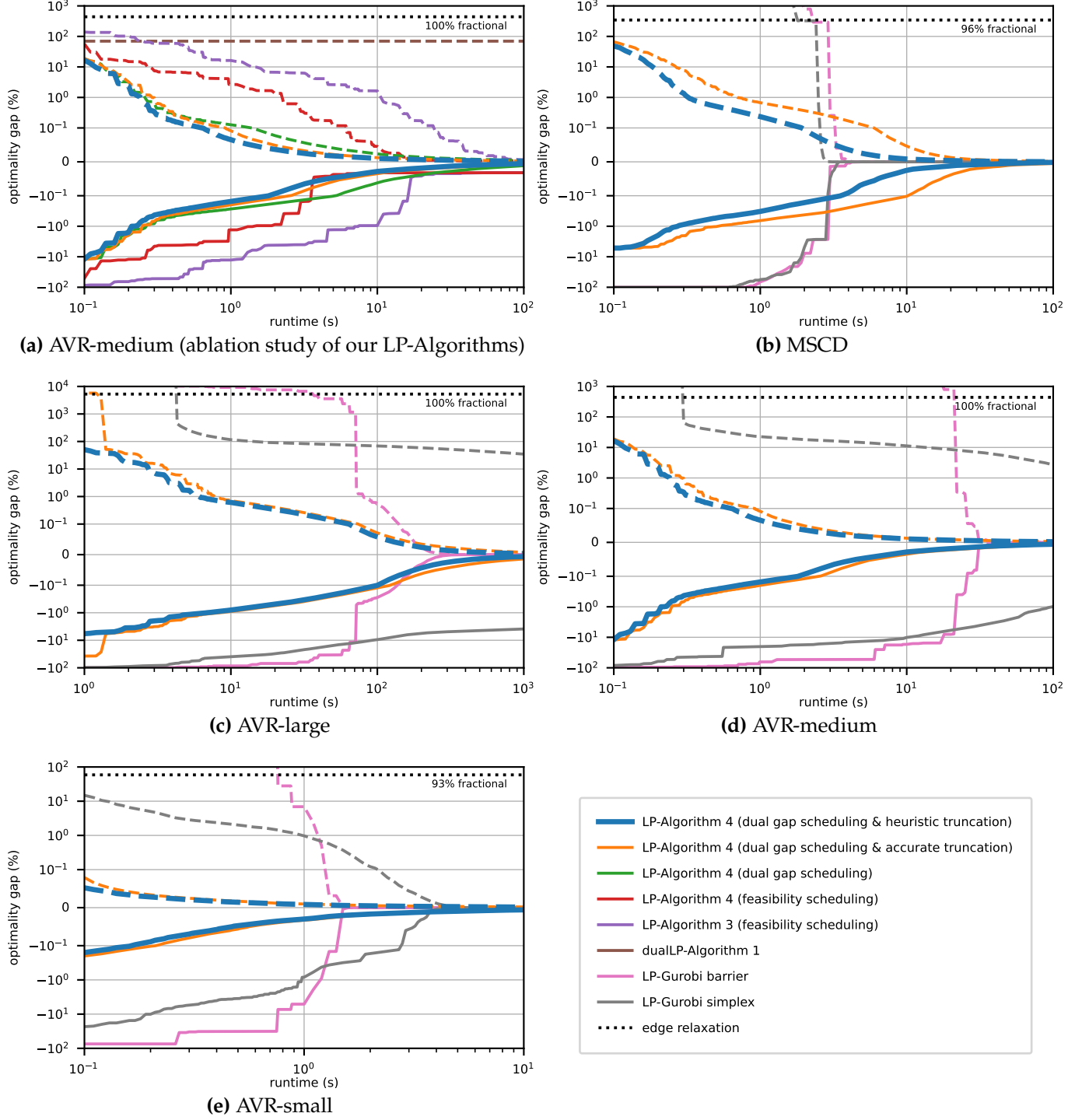


**Figure 1: Optimization of the problem relaxation.** These plots track the relative gap to the optimum of the LP relaxation of MWIS problem (2) across run time. Dashed lines refer to the dual objective (upper bound) and solid lines refer to the primal (relaxed) objective (lower bound). Instead of individual models, we show the mean objective across all models of the dataset group, providing a consolidated view of algorithm performance. Our algorithms are able to provide high-quality solutions (< 1 % rel. gap) for the majority of the instances within 1–10 seconds.

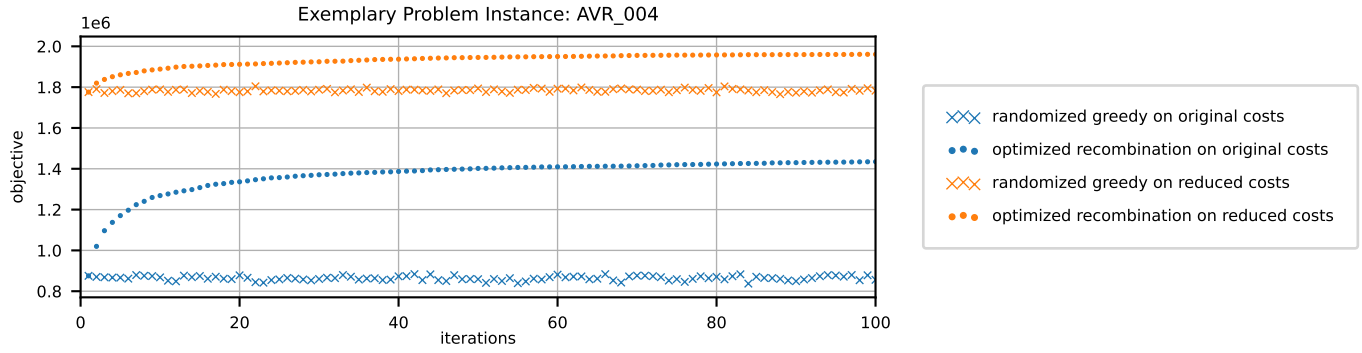


**Figure 2: Primal heuristic ablation.** Exemplary comparison on the problem instance *AVR\_004* from the *AVR-large* dataset. As the comparison suggests, optimized recombination leads to significant improvement of the resulting solution. Even more improvement is obtained due to usage of the reduced costs: Even the best recombination result obtained for the original costs is worse than each single greedily generated solution based on reduced costs.

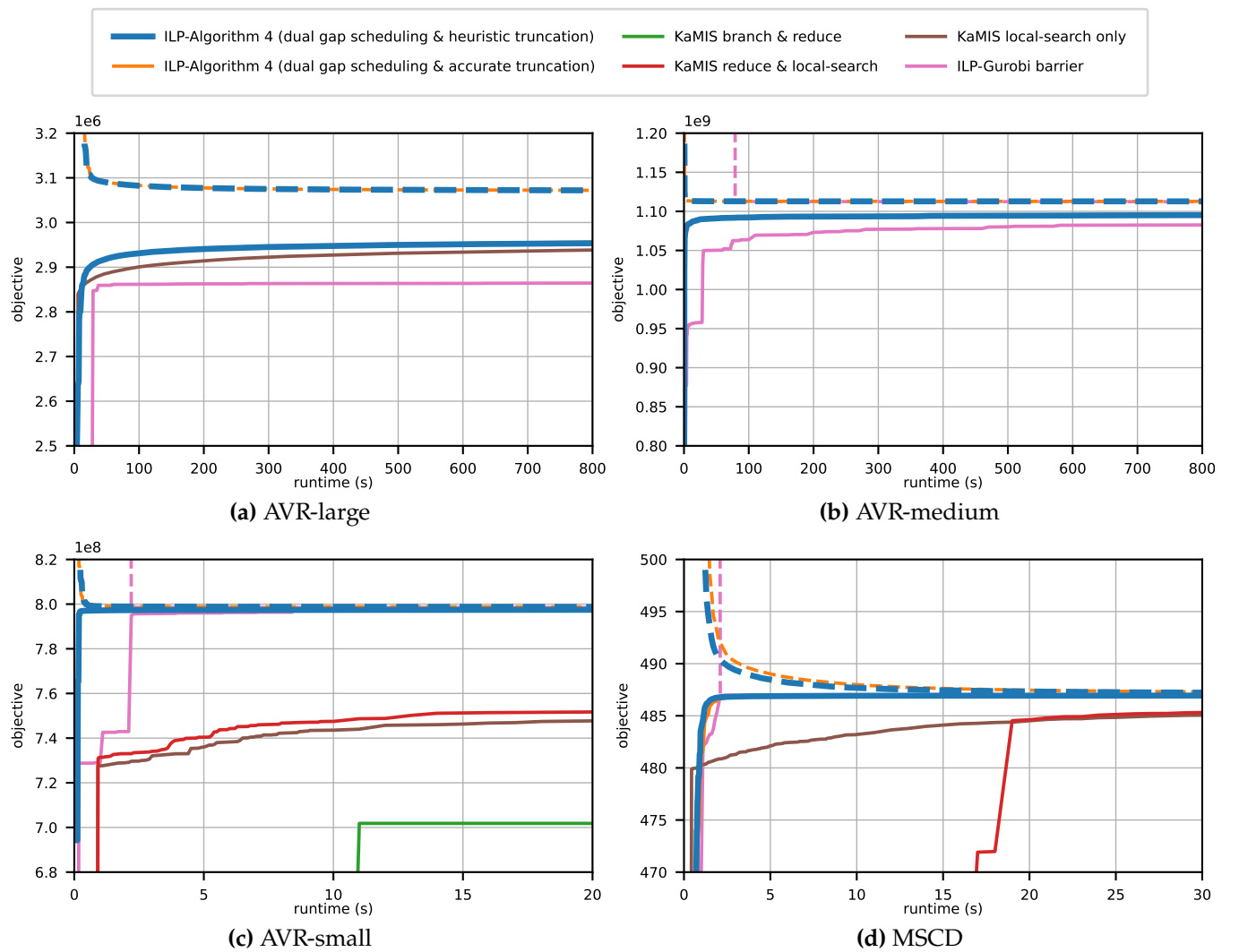


**Figure 3: Optimization of the non-relaxed problem.** This plot presents the absolute primal objective values over run time, highlighting the effectiveness of our best-performing dual optimizer in conjunction with the proposed primal heuristics. Dashed lines refer to the dual objective (upper bound) and solid lines refer to the primal objective (lower bound). We compare our solver to Gurobi ILP and KaMIS. Similarly to Figure 1 we show the mean objective across all models of the different groups. Our solver yields high-quality MWIS solutions after only a few seconds for the majority of instances. Several variants of the *KaMIS* algorithms are missing in some plots as their attained values lie outside the visible area of the respective plots.

The dual bound corresponding to the edge relaxation is given as a baseline. This baseline turned out to be very loose in *all* datasets (see also Figure 1(b-e)). On average the respective solutions had 95 % fractional values (the median value is even 99.4 %), which would not allow to use their persistency property to significantly decrease the size of the respective graphs.

The second baseline is given by *dualLP-Algorithm 1*. Although its attained bound is much better than those of the edge relaxation, it is still very much inferior to the bounds attained by other algorithms.

As expected, switching from *log*- to *exp*-domain, i.e., from *LP-Algorithm 3* (*feasibility scheduling*) to *LP-Algorithm 4* (*feasibility scheduling*), brings a significant, almost a factor of magnitude, speedup.

Further significant speedup is obtained when switching from the *feasibility*- to *dual gap* scheduling, i.e., from *LP-Algorithm 4* (*feasibility scheduling*) to *LP-Algorithm 4* (*dual gap scheduling*). One would be able to speed-up *LP-Algorithm 4* (*feasibility scheduling*) by using a larger value of the feasibility threshold  $\tau_{\text{feas}}$  (see (19)), however, it would hinder its overall convergence to the relaxed optimum at the end. This happens due to the sub-optimal starting point after the temperature drop and, therefore, the very slow convergence (numerically no convergence) at lower temperatures. In contrast, dual gap scheduling adopts the temperature dynamically to the accuracy of the attained solution.

Finally, both *heuristic* and *accurate truncations* bring another speed-up to the whole algorithm, see *LP-Algorithm 4* (*duality gap scheduling & heuristic/accurate truncation*). We discuss their behavior in more details in the description of the next experiment provided below.

**Our best methods against Gurobi in LP mode (Figure 1(b-e)).** Our next experiment compares the performance of our best LP methods *LP-Algorithm 4* (*duality gap scheduling & heuristic/accurate truncation*) against *LP-Gurobi simplex/barrier*. We do this with the same averaged plots as Figure 1(a).

The plots show that our methods significantly outperform Gurobi at the early optimization stages, but require much longer than *LP-Gurobi barrier* if a high accuracy is required. This is, however, a standard behavior of all first order methods including ours, due to their in total sub-linear (more precisely, exponentially low) convergence rate.

Although *heuristic truncation* is always somewhat faster than the *accurate* one in *LP-Algorithm 4* (*duality gap scheduling & \*\*\**), the difference is negligible in all datasets but *MSCD*. This is because instances of this datasets require stabilization more often, especially, when the relatively small stabilization threshold  $\tau_{\text{stab}} = 10$  (see Algorithm 4) is used, as it is the case for the *accurate truncation*. This is the reason why we use the much higher value  $\tau_{\text{stab}} = 10^{30}$  for all other algorithms.

Notably, *LP-Gurobi barrier* significantly outperforms *LP-Gurobi simplex* on all datasets but *MSCD* (for the latter their performance is comparable), hence we stick to *LP-Gurobi barrier* for further experiments in the ILP mode.

**Ablation study for our primal heuristic (Figure 2).** In our third experiment we show importance of the optimized recombination and usage of the reduced costs instead of the original ones. This phenomenon is not unique to this specific example and similar results can be observed for most problem instances.

As shown in Figure 2, optimized recombination leads to a significant improvement of the resulting solution. Even more improvement is obtained due to the usage of the reduced costs: Even the best recombination result obtained for the original costs is worse than each single greedily generated solution based on reduced costs.

**Our best methods against competitors in ILP mode (Figure 3).** Finally, we compare different methods addressing the non-relaxed MWIS problem (2). As with Figure 1, we show averaged plots and state their qualitative similarity to individual plots within each dataset. From our algorithms we show only *ILP-Algorithm 4* (*duality gap scheduling & heuristic/accurate truncation*) due to the best performance for the relaxed problem.

In the short run our algorithms outperforms all its competitors on all datasets but *MSCD*, where results in terms of the primal integer solution is on par with *ILP-Gurobi barrier*. In general *ILP-Gurobi barrier* is the most competitive among evaluated methods. Only *KaMIS local search only* was able to show better results and only for the *AVR-large* dataset. On all other datasets all *KaMIS \*\*\** algorithms are noncompetitive, at least in the considered time span.

On the small-sized datasets *AVR-small* and *MSCD* the comparison between our *ILP-Algorithm 4* (*duality gap scheduling & heuristic/accurate truncation*) and *ILP-Gurobi barrier* leads to similar results as for the comparison in the LP mode, see Figure 1. Namely, our methods is faster at the beginning, finds a good approximate solution very fast, but does not converge to the ILP optimum. In turn, *ILP-Gurobi barrier* is somewhat slower at the beginning, but at some point finds the ILP optimum.

However, for larger datasets *AVR-large* and *AVR-medium* *ILP-Gurobi barrier* is not always able to find the optimum and often is even unable to reach the solution accuracy of our methods within 1000 seconds.

This type of performance is quite typical, when exact methods like *ILP-Gurobi barrier* are compared to approximate ones like ours. Solid performance of our method we explain by the boost given by the reduced costs obtained with the dual optimization. Being very important for the performance of the primal heuristic at the beginning, its effect diminishes as one gets closer to the solution of the relaxed problem. In other

Dataset	Instance	Our (3600 sec)		"Cold" (c.f. [7, Tab. 2])		"Warm" (c.f. [7, Tab. 3])			
		Objective	LP-Gap 0.1% t, sec	ILSVND t, sec	METAMIS t, sec	ILSVND t, sec	METAMIS t, sec	METAMIS+LP * t, sec	
AVR-LARGE	CR-S-L-1	<b>5 653 748</b>	309	4	63	424	—	—	
	CR-S-L-2	<b>5 737 640</b>	289	12	198	590	—	—	
	CR-S-L-4	<b>5 734 265</b>	297	8	113	672	—	—	
	CR-S-L-6	<b>3 909 318</b>	110	6	34	1 840	—	—	
	CR-S-L-7	<b>2 011 084</b>	19	2	15	507	—	—	
	CR-T-C-1	<b>4 723 108</b>	50	2	13	122	—	—	
	CR-T-C-2	<b>4 945 899</b>	122	2	22	166	—	—	
	CR-T-D-4	<b>4 881 646</b>	170	2	34	583	—	—	
	CR-T-D-6	<b>3 013 249</b>	75	1	11	290	—	—	
	CR-T-D-7	<b>1 455 976</b>	10	< 1	3	—	—	—	
	CW-S-L-1	<b>1 648 272</b>	190	13	85	—	—	—	
	CW-S-L-2	<b>1 722 290</b>	186	25	148	—	—	—	
	CW-S-L-4	<b>1 733 085</b>	133	36	463	—	—	—	
	CW-S-L-6	<b>1 164 850</b>	35	9	137	—	—	—	
	CW-S-L-7	<b>589 334</b>	10	7	90	—	—	—	
AVR-MEDIUM	CW-T-C-1	<b>1 330 362</b>	15	6	39	1 016	—	—	
	CW-T-C-2	<b>937 013</b>	14	10	206	—	—	—	
AVR-MEDIUM	CW-T-D-4	<b>460 198</b>	2	1	6	56	—	—	
	CW-T-D-6	<b>459 776</b>	2	< 1	7	28	—	—	
	MR-D-03	<b>1 758 074 154</b>	1	< 1	< 1	< 1	18	80	
	MR-D-05	<b>1 790 179 623</b>	1	< 1	1	< 1	2	8	
	MR-D-FN	<b>1 802 268 039</b>	1	< 1	1	< 1	3	8	
	MR-W-FN	<b>5 386 842 781</b>	< 1	< 1	< 1	< 1	< 1	< 1	
	MT-D-200	<b>287 155 108</b>	< 1	< 1	< 1	< 1	< 1	< 1	
	MT-D-FN	290 866 943	< 1	< 1	165	< 1	< 1	< 1	
	MT-W-200	<b>384 056 012</b>	< 1	< 1	< 1	< 1	< 1	< 1	
	MT-W-FN	<b>390 869 891</b>	< 1	< 1	< 1	< 1	< 1	< 1	
	MW-D-20	<b>526 688 093</b>	< 1	< 1	1	< 1	1	2	
	MW-D-40	<b>538 944 498</b>	< 1	< 1	2	< 1	1	3	
	MW-D-FN	<b>545 720 496</b>	< 1	< 1	< 1	< 1	4	6	
	MW-W-05	<b>1 329 653 408</b>	18	1 699	1 699	1 699	1 699	1 699	
	MW-W-10	1 300 124 841	18	—	—	—	—	—	
	MW-W-FN	1 248 553 336	17	—	—	—	—	—	
AVR-SMALL	MR-D-01	<b>1 691 358 724</b>	< 1	< 1	1	< 1	< 1	< 1	
	MT-D-01	238 166 485	< 1	< 1	< 1	< 1	< 1	< 1	
	MT-W-01	312 121 568	< 1	< 1	< 1	< 1	< 1	< 1	
	MW-D-01	<b>476 361 236</b>	< 1	18	141	3	18	18	
	MW-W-01	1 270 305 952	< 1	< 1	< 1	< 1	< 1	< 1	

**Table 2:** Comparison of *ILP-Algorithm 4* (duality gap scheduling & heuristic truncation) denoted as *Our* to METAMIS [7] and ILSVND [24] based on [7, Tab. 2, 3]. Datasets are sorted by their size, from the largest on top to the smallest in the bottom. "Warm" and "Cold" columns correspond to algorithms that use or, respectively, do not use a warm-start with a specific (unpublished and unknown to us) initial solution as explained in [7]. **LP-Gap 0.1%** – time required to attain the 0.1% relative duality gap for the relaxed problem. **ILSVND**, **METAMIS**, **METAMIS+LP** – time required by *Our* primal heuristic to attain the best value of the respective algorithm (corresponds to the column "w" in [7, Tab. 2, 3]). To obtain the full time of *Our* algorithm this value should be added to the respective value in the "LP-Gap 0.1%" column. Objective value marked as **bold** means that this is *strictly greater* than those obtained by any competing algorithm with the "Cold"-start. *Italic* font means that our value and value of the best competing algorithm coincide: For two of them, MT-D-01 and MT-W-01, this value furthermore coincides with the LP bound and is, therefore, optimal. Although *Our* method only uses a comparably simple primal heuristics, it outperforms its competitors due to the usage of the reduced costs, see a detailed explanation in the main text.

words, primal heuristics are typically unable to fully exploit high-precision relaxed solutions, in contrast to the branch-and-bound employed by Gurobi.

**Comparison to METAMIS [7] and ILSVND [24]** state-of-the-art primal heuristics on the *AVR-\*\*\** dataset is given in Table 2. To this end we follow the setting of [7] and run the fastest variant of *Our* method, *ILP-Algorithm 4 (duality gap scheduling & heuristic truncation)*, 5 times with different random seeds for 3600 seconds, exactly like the algorithms we compare to were run by authors of [7]. Similarly, the result of the best run is reported for each problem instance.

To separate runtime contribution of our dual method from those of the primal heuristic, we first run the dual updates until the 0.1% relative duality gap for the relaxed LP is attained and only afterwards start running primal updates in each batch additionally. Typically, due to sparsity, the time needed by dual updates after attaining the above duality gap constitutes less than 5% of the time required by the primal heuristic and, therefore, can be largely ignored.

Table 2 shows the time required by our method to attain or overcome the results of the competing algorithms. Following [7], we consider the competing algorithms with "cold" and "warm"-start. The latter uses an unpublished and, therefore, unknown to us initial solution. We refer to [7] for further details and actual objective values attained by the METAMIS and ILSVND algorithms.

As can be seen from Table 2, for all but two datasets (MW-W-10 and MW-W-FN) our method finds better or the same accuracy solutions as the competitors with "cold" start. For most of instances of *AVR-medium* and *AVR-small* this happens within 1 second, few require up to 7 seconds and only three instances – more than 100 seconds after attaining the 0.1% duality gap for the relaxed problem. Finding better solutions than METAMIS for instances from *AVR-large* requires less than 100 seconds for 11 problem instances of of 17, and at most 206 seconds for each of the rest 6 instances. Note that according to [7] METAMIS as well as ILSVND did not converge in 3600 seconds "on larger instances" (we assume *AVR-large*) and, essentially required that time to attain their best solutions. Additionally, our algorithm attains the best objective values of ILSVND *significantly* faster than METAMIS, c.f. [7][Tab. 2, column METAMIS- $t^*[s]$ ].

Moreover, for most of *AVR-medium* and *AVR-small* problem instances, *Our* method has been even able to outperform all its competitors that used a "warm"-start initial solution, unpublished and unknown to us, and, therefore, not used in *Our* algorithm. In the experiments of [7], this "warm"-start initial solution lead to significant improvement of the results of both, METAMIS and ILSVND algorithms. The METAMIS+LP additionally to the initial solution uses the primal LP solution to guide its local search.

So, the question arises, *how it comes that Our method outperforms METAMIS that employs a much stronger primal heuristic?* We believe, this is the usage of the reduced costs instead of the original ones that really makes the difference. This is clearly demonstrated for our primal heuristic in Figure 2. Unfortunately, as mentioned in Section 9.1, to use reduced costs with the MWIS problem one has to adjust primal heuristics, moreover, some of them cannot even be used at all. This fact prevented us from running KaMIS and ILSVND algorithms (code of METAMIS is not published) with reduced costs to additionally substantiate our statement.

## 11 Conclusions

We presented a new method to address the maximum-weight independent set problem. The key component of the method is an approximate solver for the clique cover LP relaxation. The usage of the reduced costs allows to simplify and speed-up the primal heuristic, which, in turn, leads to a competitive approximate solver of the non-relaxed problem. The advantages of our method are best seen on large-scale problem instances.

We expect our method to become even more competitive when used with more powerful primal heuristics that additionally include local search as a subroutine.

## 12 Acknowledgments

We thank Prof. Bernhard Schmitzer for an insightful discussion about modern advances in computational optimal transport. The discussion lead to the decisive speedup of our algorithms described in this work. A special thanks to Prof. Paul Swoboda for thorough proofreading and numerous comments that notably improved this paper. This work was supported by the German Research Foundation projects 498181230 and 539435352. Authors further acknowledge facilities for high throughput calculations bwHPC of the state of Baden-Württemberg (DFG grant INST 35/1597-1 FUGG) as well as Center for Information Services and High Performance Computing (ZIH) at TU Dresden.

## References

- [1] Amazon. <http://www.amazon.com>.
- [2] Dimitri P. Bertsekas. Nonlinear programming, second edition. Athena scientific, 1999.
- [3] Endre Boros and Peter L. Hammer. Pseudo-boolean optimization. *Discrete applied mathematics*, 123(1-3):155–225, 2002.

- [4] Lev M. Bregman. The Relaxation Method of Finding the Common Point of Convex Sets and its Application to the Solution of Problems in Convex Programming. *USSR Computational Mathematics and Mathematical Physics*, 1967.
- [5] William Brendel and Sinisa Todorovic. Segmentation as maximum-weight independent set. In *Advances in Neural Information Processing Systems*, 2010.
- [6] Tomáš Dlask and Bogdan Savchynskyy. Relative-Interior Solution for (Incomplete) Linear Assignment Problem with Applications to Quadratic Assignment Problem. *arXiv preprint arXiv:2301.11201*, 2023.
- [7] Yuanyuan Dong, Andrew V. Goldberg, Alexander Noe, Nikos Parotsidis, Mauricio G.C. Resende, and Quico Spaen. A Local Search Algorithm for Large Maximum Weight Independent Set Problems. In *30th Annual European Symposium on Algorithms (ESA 2022)*. Schloss-Dagstuhl-Leibniz Zentrum für Informatik, 2022.
- [8] Yuanyuan Dong, Andrew V. Goldberg, Alexander Noe, Nikos Parotsidis, Mauricio G.C. Resende, and Quico Spaen. New instances for maximum weight independent set from a vehicle routing application. In *Operations Research Forum*, volume 2, pages 1–6. Springer, 2021.
- [9] Anton Eremeev and Julia Kovalenko. Optimal recombination in genetic algorithms for combinatorial optimization problems: Part I. *Yugoslav Journal of Operations Research*, 24(1):1–20, 2014.
- [10] Shu-Cherng Fang, Jay R. Rajasekera, and H.-S. Jacob Tsao. *Entropy optimization and mathematical programming*, volume 8. Springer Science & Business Media, 2012.
- [11] Michael R. Garey and David S. Johnson. *Computers and intractability*. W. H. Freeman and Company, New York, 1979.
- [12] Ernestine Großmann, Sebastian Lamm, Christian Schulz, and Darren Strash. Finding near-optimal weight independent sets at scale. In *Proceedings of the Genetic and Evolutionary Computation Conference*, pages 293–302, 2023.
- [13] Martin Grötschel, László Lovász, and Alexander Schrijver. Polynomial algorithms for perfect graphs. In *North-Holland mathematics studies*. Volume 88, pages 325–356. Elsevier, 1984.
- [14] Gurobi. Gurobi Optimization, 2018. <http://www.gurobi.com>.
- [15] Stefan Haller, Lorenz Feineis, Lisa Hutschenreiter, Florian Bernard, Carsten Rother, Dagmar Kainmüller, Paul Swoboda, and Bogdan Savchynskyy. A comparative study of graph matching algorithms in computer vision. In *European Conference on Computer Vision*, pages 636–653. Springer, 2022.
- [16] Dorit Hochbaum. Approximating covering and packing problems: set cover, vertex cover, independent set, and related problems. In *Approximation algorithms for NP-hard problems*, pages 94–143. 1996.
- [17] Akihisa Kako, Takao Ono, Tomio Hirata, and Magnús M. Halldórsson. Approximation algorithms for the weighted independent set problem. In *Graph-Theoretic Concepts in Computer Science: 31st International Workshop, WG 2005, Metz, France, June 23–25, 2005, Revised Selected Papers 31*, pages 341–350. Springer, 2005.
- [18] KaMIS - Karlsruhe Maximum Independent Sets. <https://karlsruhemis.github.io/>.
- [19] Richard M. Karp. Reducibility among combinatorial problems. In *Complexity of computer computations*. Springer, 1972.
- [20] Yam Kushinsky, Haggai Maron, Nadav Dym, and Yaron Lipman. Sinkhorn algorithm for lifted assignment problems. *SIAM Journal on Imaging Sciences*, 12(2):716–735, 2019.
- [21] Sebastian Lamm, Christian Schulz, Darren Strash, Robert Williger, and Huashuo Zhang. Exactly solving the maximum weight independent set problem on large real-world graphs. In *2019 Proceedings of the Twenty-First Workshop on Algorithm Engineering and Experiments (ALENEX)*, pages 144–158. SIAM, 2019.
- [22] John W. Moon and Leo Moser. On cliques in graphs. *Israel journal of Mathematics*, 3:23–28, 1965.
- [23] George L. Nemhauser and Leslie E. Trotter Jr. Vertex packings: Structural properties and algorithms. *Mathematical Programming*, 8(1):232–248, 1975.
- [24] Bruno Nogueira, Rian G.S. Pinheiro, and Anand Subramanian. A hybrid iterated local search heuristic for the maximum weight independent set problem. *Optimization Letters*, 12:567–583, 2018.
- [25] Vangelis T. Paschos. A survey of approximately optimal solutions to some covering and packing problems. *ACM Computing Surveys (CSUR)*, 29(2):171–209, 1997.
- [26] Gabriel Peyré, Marco Cuturi, et al. Computational optimal transport. *Center for Research in Economics and Statistics Working Papers*, (2017-86), 2017.

- [27] Mangal Prakash. Fully Unsupervised Image Denoising, Diversity Denoising and Image Segmentation with Limited Annotations. PhD thesis, Technische Universität Dresden, 2022.
- [28] Daniel Průša and Tomáš Werner. Solving LP relaxations of some NP-hard problems is as hard as solving any linear program. *SIAM Journal on Optimization*, 29(3):1745–1771, 2019.
- [29] Wayne Pullan. Optimisation of unweighted /weighted maximum independent sets and minimum vertex covers. *Discrete Optimization*, 6(2):214–219, 2009.
- [30] Elisabeth Rodriguez-Heck, Karl Stickler, Matthias Walter, and Stefan Weltge. Persistency of Linear Programming Formulations for the Stable Set Problem. *Mathematical programming*, 192:387–407, 1, 2022/3.
- [31] Carsten Rother, Vladimir Kolmogorov, Victor S. Lempitsky, and Martin Szummer. Optimizing Binary MRFs via Extended Roof Duality. In *Proceedings of the IEEE Conference on Computer Vision and Pattern Recognition*, 2007.
- [32] Sujay Sanghavi, Devavrat Shah, and Alan Willsky. Message passing for max-weight independent set. *Advances in Neural Information Processing Systems*, 20, 2007.
- [33] Bogdan Savchynskyy. Discrete Graphical Models – An Optimization Perspective. *Foundations and Trends in Computer Graphics and Vision*, 2019.
- [34] Bernhard Schmitzer. Stabilized sparse scaling algorithms for entropy regularized transport problems. *arXiv Preprint arXiv:1610.06519v1*, 2016.
- [35] Bernhard Schmitzer. Stabilized sparse scaling algorithms for entropy regularized transport problems. *SIAM Journal on Scientific Computing*, 41(3):A1443–A1481, 2019.
- [36] Alexander Schrijver. Combinatorial optimization: polyhedra and efficiency, volume 24 of number 2. Springer, 2003.
- [37] Devavrat Shah. Max product for max-weight independent set and matching. *arXiv preprint cs/0508097*, 2005.
- [38] Richard Sinkhorn. A Relationship Between Arbitrary Positive Matrices and Doubly Stochastic Matrices. *The Annals of Mathematical Statistics*, 1964.
- [39] Source code of algorithms for minimizing functions of binary variables with unary and pairwise terms based on roof duality by Vladimir Kolmogorov. <https://pub.ista.ac.at/~vnk/software/QPBO-v1.4.src.zip>.
- [40] Luca Trevisan. Inapproximability of combinatorial optimization problems. *Paradigms of Combinatorial Optimization: Problems and New Approaches*:381–434, 2014.
- [41] Jonathan Weed. An explicit analysis of the entropic penalty in linear programming. In *Conference On Learning Theory*, pages 1841–1855. PMLR, 2018.

## 13 Appendix

### Transformation of the recombination problem (Section 9) into quadratic pseudo-boolean maximization

Let  $\mathcal{V}'$  stand for the set of graph nodes that differ in two feasible solutions  $\mathbf{x}^1, \mathbf{x}^2 \in \{0, 1\}^n$  of the MWIS problem (1) to be fused, i.e.,  $x_i^1 = \bar{x}_i^2, i \in \mathcal{V}'$  and  $x_i^1 = x_i^2$  for  $i \in \mathcal{V} \setminus \mathcal{V}'$  respectively. Let  $\mathbf{c}$  be the cost vector of the problem. Let also the set of edges  $\mathcal{E}'$  be inherited from the initial problem:  $\mathcal{E}' = \{\{i, j\} \in \mathcal{E} : i, j \in \mathcal{V}'\}$ . By construction, the graph  $(\mathcal{V}', \mathcal{E}')$  is bipartite, that is  $\mathcal{E}' \subseteq \mathcal{V}^1 \times \mathcal{V}^2$ , where  $\mathcal{V}' = \mathcal{V}^1 \cup \mathcal{V}^2$ ,  $\mathcal{V}^1 \cap \mathcal{V}^2 = \emptyset$ ,  $\mathcal{V}^k = \{i \in \mathcal{V}' : x_i^k = 1\}$ ,  $k = 1, 2$ . For the sake of notation we assume the edges to be oriented, e.g.,  $(i, i') \in \mathcal{E}'$  implies  $i \in \mathcal{V}^1$  and  $i' \in \mathcal{V}^2$ .

Consider the variable substitution

$$\forall i \in \mathcal{V}' : (y_i, w_i) := \begin{cases} (x_i, c_i), & i \in \mathcal{V}^1 \\ (\bar{x}_i, -c_i), & i \in \mathcal{V}^2 \end{cases} \quad (30)$$

Then for any  $i \in \mathcal{V}^2$  and binary  $x_i$  it holds  $c_i x_i = w_i y_i - w_i$ . This turns the quadratic pseudo-boolean representation (5) of the considered MWIS problem into the so called *oriented form* [33, Ch. 11] as follows:

$$\begin{aligned} & \sum_{i \in \mathcal{V}'} c_i x_i - M \cdot \sum_{(i,j) \in \mathcal{E}'} x_i x_j \\ &= - \sum_{l \in \mathcal{V}^2} w_l + \sum_{i \in \mathcal{V}'} w_i y_i - M \cdot \sum_{(i,l) \in \mathcal{E}'} y_i \bar{y}_l. \end{aligned} \quad (31)$$

As shown in, e.g., in [33, Ch. 11], maximization of the right-hand-side of (31) reduces to the min-st-cut and we used the software [39] that implements this reduction and solves the respective min-st-cut problem.

**Proof of Proposition 1.** Due to half-integrality, it is sufficient to consider only half-integer feasible solutions. Due to the cost non-negativity the feasible solution  $\mathbf{y} = (\underbrace{\frac{1}{2}, \frac{1}{2}, \dots, \frac{1}{2}}_n)$  is the best among those with coordinates 1/2 and 0 only, as it contains the maximal number of non-zero coordinates. The cost of this solution is  $\langle \mathbf{c}, \mathbf{y} \rangle = \frac{1}{2} \sum_{j \in \mathcal{V}} c_j$ .

Consider now feasible solutions that are at least one coordinate equal to 1. Since the graph is fully-connected, there are only  $|\mathcal{V}'|$  of them, e.g., those of the form  $x^i = (\underbrace{0, \dots, 0}_{i-1}, i, 0, \dots, 0)$  with the total costs equal to  $c_i$ , respectively. The condition of the proposition implies

$$c_i < \sum_{j \in \mathcal{V} \setminus \{i\}} c_j = \sum_{j \in \mathcal{V}} c_j - c_i \quad (32)$$

and, therefore,  $c_i < \frac{1}{2} \sum_{j \in \mathcal{V}} c_j = \langle \mathbf{c}, \mathbf{y} \rangle$ .  $\square$

**Proof of Proposition 2.** The proof is a direct consequence of the fact that for any  $\mathbf{x} \in [0, 1]^n$  an inequality  $\sum_{i \in K_l} x_i \leq 1$  implies  $\sum_{i \in K'_l} x_i \leq 1$  as long as  $K'_l \subseteq K_l$ .  $\square$

**Proof of Proposition 3.** It is sufficient to prove that the feasible set being a polytope has only integer vertices. Indeed, assume  $\mathbf{x}' \in [0, 1]^n$  is a vertex. Then there is  $\mathbf{c} \in \mathbb{R}^n$  such that  $\mathbf{x}'$  is a unique solution of  $\{\max_{\mathbf{x} \in [0, 1]^n} \langle \mathbf{c}, \mathbf{x} \rangle, \text{ s.t. } \sum_{i=1}^n x_i \leq 1\}$ . Assume that  $\mathbf{x}'$  is fractional and w.l.o.g.  $c_1 \geq c_2 > 0$  and  $x'_1, x'_2 > 0$ . Then

$$\begin{aligned} \langle \mathbf{c}, \mathbf{x}' \rangle &= c_1 x'_1 + c_2 x'_2 + \sum_{i=3}^n c_i x'_i \\ &\leq c_1(x'_1 + x'_2) + c_2 \cdot 0 + \sum_{i=3}^n c_i x'_i = \langle \mathbf{c}, \mathbf{x}'' \rangle, \end{aligned} \quad (33)$$

where  $\mathbf{x}''$  such that  $x''_1 = x'_1 + x'_2$ ,  $x''_2 = 0$  and  $x''_i = x'_i$  for  $i = 3 \dots n$ .  $\mathbf{x}''$  is feasible since  $\mathbf{x}'$  is feasible as vertex. If the inequality in (33) holds strictly, then  $\mathbf{x}'$  is not a solution and if it holds as equality, then  $\mathbf{x}'$  is not a unique one. So we obtained a contradiction.  $\square$

**Proof of Proposition 4.** The condition  $\frac{\partial D}{\partial \lambda_j}[\mathbf{x}^*] = 0$  for all  $j \in [m]$  together with (9) implies feasibility of  $\mathbf{x}^*$  and optimality of  $\lambda$ . Therefore, for any  $\mathbf{x}$  feasible for (3) it holds

$$\langle \mathbf{c}, \mathbf{x} \rangle \leq D(\lambda) = \sum_{j=1}^m \lambda_j + \langle \mathbf{c}^\lambda, \mathbf{x}^* \rangle = \langle \mathbf{c}, \mathbf{x}^* \rangle, \quad (34)$$

and thus,  $\mathbf{x}^*$  is an optimal solution of (3). If additionally  $\mathbf{x}^*$  is integer, inequality (34) proves its optimality for the non-relaxed problem (2) as well.  $\square$

**Proof of Lemma 1.** The proof directly follows from the fact that every time the value of  $x_i, i \in [n+m]$ , changes, it is divided by a value  $s \geq x_i$ .  $\square$

**Proof of Proposition 5.** Algorithm 2 is a special case of the algorithm that converges to the optimum of  $\{\max_{\mathbf{x} \geq 0} \langle \mathbf{c}, \mathbf{x} \rangle + T\mathcal{H}(\mathbf{x}), \text{ s.t. } A\mathbf{x} = \mathbf{b}\}$  described in [4, P. 215-216]. In particular:

- Initial value of  $\mathbf{x}$  is selected as an unconstrained maximum of the objective function. Indeed,

$$0 = (\langle \mathbf{c}, \mathbf{x} \rangle + T\mathcal{H}(\mathbf{x}))' = \mathbf{c} - T \log \mathbf{x}. \quad (35)$$

This implies  $\mathbf{x} = \exp(\mathbf{c}/T)$ .

- According to [4, Eq.(2.34), (2.35)], the update rule has a form

$$x'_i := x_i \exp(\gamma a_{ij}/T), \quad (36)$$

where  $\gamma$  is computed as a solution of

$$\sum_{i=1}^{n+m} a_{ij} x_i \exp(\gamma a_{ij}/T) = b_j. \quad (37)$$

Here the matrix  $A = (a_{ij})$  and vector  $\mathbf{b} = (b_j)$  define constraints  $A\mathbf{x} = \mathbf{b}$  of the problem,  $i$  and  $j$  are the

column and row indices respectively. In our case  $b_j = 1$  and  $a_{ij} = \llbracket i \in \bar{K}_j \rrbracket$ , where  $\llbracket B \rrbracket$  is Iverson bracket equal to 1 if  $B$  holds, otherwise 0.

Plugging the values of  $a_{ij}$  and  $b_j$  into (36) and (37) and solving the latter w.r.t.  $\gamma$  leads to the update  $x'_i = \frac{x_i}{\sum_{i \in \bar{K}_j} x_i}$ .

□

**Proof of Lemma 2.** Indeed, let  $\lambda'_k = \lambda_k$  for  $k \neq j$  and

$$\begin{aligned} \lambda'_j &:= \lambda_j + c_{i^*}^\lambda + T \log \sum_{i \in \bar{K}_j} \exp \frac{c_i^\lambda - c_{i^*}^\lambda}{T} \\ &= \lambda_j + T \log \sum_{i \in \bar{K}_j} \exp(c_i^\lambda / T). \end{aligned} \quad (38)$$

Taking in account the transformation  $\mathbf{x} = \exp(\mathbf{c}^\lambda / T)$  the elementary update in Algorithm 2 can be rewritten as

$$\begin{aligned} x'_i &:= \frac{x_i}{\sum_{i \in \bar{K}_j} x_i} = \frac{\exp(c_i^\lambda / T)}{\sum_{i \in \bar{K}_j} \exp(c_i^\lambda / T)} \\ &= \exp \left( \frac{c_i^\lambda - T \log \sum_{i \in \bar{K}_j} \exp(c_i^\lambda / T)}{T} \right) \\ &= \exp \left( \frac{c_i - \sum_{k \in J_i} \lambda_k - T \log \sum_{i \in \bar{K}_j} \exp(c_i^\lambda / T)}{T} \right) \\ &= \exp \left( \frac{c_i - \sum_{k \in J_i \setminus \{j\}} \lambda_k - (\lambda_j + T \log \sum_{i \in \bar{K}_j} \exp(c_i^\lambda / T))}{T} \right) \\ &= \exp \left( \frac{c_i - \sum_{k \in J_i} \lambda'_k}{T} \right) = \exp \left( c_i^{\lambda'} / T \right) \end{aligned} \quad (39)$$

□

**Proof of Lemma 3.** follows directly from Lemma 1 and Lemma 2. □

**Proof of Proposition 6.** The first part of the statement directly follows from the strong duality, Proposition 5 and Lemma 2. The second part follows from Lemma 7 that implies that after processing the clique  $\bar{K}_j$  it holds

$$\begin{aligned} \frac{\partial D^T}{\partial \lambda_j} &= 1 + \frac{\partial (T \sum_{i=1}^{n+m} \exp(c_i^\lambda / T))}{\partial \lambda_j} \\ &= 1 + T \sum_{i=1}^{n+m} \frac{\partial (\exp(c_i^\lambda / T))}{\partial \lambda_j} = 1 - \sum_{i \in \bar{K}_j} \exp(c_i^\lambda / T) \\ &\stackrel{\text{Lemma 2}}{=} 1 - \sum_{i \in \bar{K}_j} x_i \stackrel{\text{Algorithm 2}}{=} 0 \end{aligned} \quad (40)$$

□

**Proof of Lemma 4.** Initialization:  $\hat{\mathbf{x}}$  is feasible by construction in Line 2. Exactly two coordinates in each

inequality  $j \in J_i$  containing  $x_i$  are changing at each iteration of the loop over  $i \in [n]$  in Lines 3-7: The value of  $\hat{x}_i$  is increased (Line 5) and the value of the respective slack  $\hat{x}_{n+j}$  is decreased by the same amount. So the sum of coordinates of  $\hat{\mathbf{x}}$  in each clique constraint remains unchanged and equal to one. □

**Proof of Lemma 5.** As  $\sum_{j \in \bar{K}_j} x_i = 1$  for all  $j \in J_i$ , it holds  $M \geq x_i$  in Line 5. In turn it implies  $\hat{x}_i = x_i$ . □

**Proof of Lemma 6.** The mapping  $\mathcal{P}$  is continuous as a superposition of continuous mappings defined by Algorithm 5.

To prove the implication denote  $\hat{\mathbf{x}} := \mathcal{P}(\mathbf{x})$  and note that  $x_i \geq \hat{x}_i$  for any  $i \in [n]$  by construction. The latter inequality holds as equality and, therefore, trivially satisfies the implication, unless there exist a constraint  $j \in [m]$  such that  $\hat{x}_{n+j} = 0$ . Consider now

$$\begin{aligned} \epsilon &\geq \underbrace{\sum_{i' \in \bar{K}_j} x_{i'}}_{\leq 1+\epsilon} - \underbrace{\sum_{i' \in \bar{K}_j} \hat{x}_{i'}}_{=1} = \sum_{i' \in \bar{K}_j} \underbrace{(x_{i'} - \hat{x}_{i'})}_{\geq 0} + \underbrace{x_{n+j} - \hat{x}_{n+j}}_{\geq 0} = 0 \\ &\geq \sum_{i' \in \bar{K}_j} |x_{i'} - \hat{x}_{i'}| \stackrel{i \in K_j}{\geq} |x_i - \hat{x}_i|. \end{aligned} \quad (41)$$

□

**Proof of Lemma 7.** Consider

$$\begin{aligned} \max_{\mathbf{x} \in [0,1]^{n+m}} \langle \mathbf{c}, \mathbf{x} \rangle - T \sum_{i=1}^{n+m} (x_i \log x_i - x_i) \\ = \sum_{i=1}^{n+m} \max_{x_i \in [0,1]} c_i x_i - T x_i \log x_i + T x_i. \end{aligned} \quad (42)$$

The function  $f(x) := cx - Tx \log x + Tx$  of a scalar  $x$  dependent on scalars  $c \leq 0$  and  $T \geq 0$  is concave and therefore its optimum is defined by the following condition

$$0 = \nabla f(x) = c - T(\log x + x/x - 1) = c - T \log x. \quad (43)$$

It implies

$$\log x = c/T; \quad x = \exp(c/T). \quad (44)$$

Since  $c \leq 0$ , it holds  $0 \leq x \leq 1$ , i.e. it satisfies the box constraints constraints on  $x_i$  in (42).

The value of  $f(x)$  in its maximum is computed as

$$\begin{aligned} \max_{x \in [0,1]} f(x) &= c \cdot \exp(c/T) - T \cdot \exp(c/T)(c/T) + T \exp(c/T) \\ &= T \cdot \exp(c/T). \end{aligned} \quad (45)$$

Putting all together leads to (24). □